UNIVERSITY OF NAPLES FEDERICO II

Department of Structures for Engineering and Architecture

PH.D. PROGRAMME IN SEISMIC RISK

COORDINATOR PROF. ALDO ZOLLO

XXVI CYCLE

BARBARA POLIDORO

PH.D. THESIS

Some seismic-cluster-based models for risk analysis of structures

TUTOR PROF. IUNIO IERVOLINO

YEAR 2014

Ai miei genitori,

ad Andrea e a Marco

TABLE OF CONTENTS

LIST OF FIGURES

Chapter 1 - INTRODUCTION

1.1. Background and motivations

Seismic risk may be defined as the probability that a pre-defined level of loss for a specific structure due to earthquakes is exceeded within a time period of interest. It is a function of three main components: the seismic hazard, the seismic vulnerability and the exposure.

Seismic hazard accounts for the probability of exceedance of a ground motion intensity measure at a site of interest in a given period.

Seismic vulnerability refers to, instead, the probability of reaching a certain damage level given an intensity measure.

Exposure represents the probability of exceedance of an economic loss given a damage level reached by the structure.

A sound methodology for identifying and analyzing all details of the problem has been proposed by the Pacific Earthquake Engineering Research (PEER) Center and it is named Performance-Based Earthquake Engineering (PBEE; Cornell and Krawinkler, 2000).

The performance assessment and the design process used to evaluate the seismic risk is divided into four steps, Figure (1.1), consisting of quantifying the seismic ground motion hazard, assessing the structural response, estimating the damage to building and content and resulting consequences in terms of financial losses, fatalities and business interruption. Such an approach presents the advantage of separating the computation of seismic risk into different discipline-specific contributions (engineering seismology, structural engineering, cost analysis, decision making). This four independent "modules" are then linked together through intermediate output variables, i.e., Intensity Measures (IMs), Engineering Demand Parameters (EDPs) and Damage Measures (DMs).

Figure 1.1. Schematic illustration of the Performance-Based Earthquake Engineering framework and the "link" variables IM, EDP and DM.

In the first phase, that is, the hazard analysis, the annual rate of exceedance of a ground motion intensity measure (IM) at a site is evaluated. The last one is also known as the hazard curve and it can be obtained from a conventional Probabilistic Seismic Hazard Analysis (PSHA; McGuire, 2004) that will be reviewed in the next section.

In the structural analysis phase, an analytical modeling of the building is performed to obtain the Engineering Demand Parameter. This is a structural response parameter well-related to damage of structural and non-structural components and content of the structure. Examples of suitable EDPs are the interstorey drift or force demands to structural members, or in general, structural parameters that allow to control the state of the structure up to collapse. The relationship between EDPs and IMs is typically obtained through inelastic dynamic analyses (IDA; Vamvatsikos and Cornell, 2002). The output of this process, which is often referred to as Probabilistic Seismic Demand Analysis (PSDA; Shome 2006), is the conditional probability that the EDP exceeds a specified value *edp*, given that the IM is equal to a particular *im*. The integration of the previous probability over the hazard curve provides the mean annual frequency of exceedance of the EDP.

In the damage analysis phase, EDPs are related to the damage measures of the building. In particular, it is possible to refer to its structural components, non-structural components or contents and for each component of interest, a Damage Measure (DM) may be defined to describe the level of damage reached during an earthquake. The output of the damage analysis is a relationship between the EDPs and the DMs expressing the probability of being in a damage state *dm*, given that the EDP is equal to a given value *edp*. Such relationships, referred to as *fragility*, are computed, in general, by means of analytical/numerical modeling, laboratory test or field experience.

In the last phase of the PEER procedure, that is loss analysis, attention is focused on the losses (i.e., decision variables DVs) due to the chosen DMs. While DMs usually

refer to components, the DVs are defined at the system or building level. If the fragility functions for all relevant damage states of all relevant components are known, the DVs of interest can be evaluated either directly or by means of cost functions that relate the damage states to costs (Yeo and Cornell, 2005).

All the procedure may be expressed as a triple integral based on the total probability theorem as shown in Equation (1.1), where the final result is the mean annual frequency (MAF), λ, of exceeding of a DV threshold (Yeo and Cornell, 2005).

$$\lambda(DV) = \iiint G(DV \mid DM) \cdot dG(DM \mid EDP) \cdot dG(EDP \mid IM) \cdot |d\lambda(IM)| \tag{1.1}$$

In the above Equation $\lambda(IM)$ is the mean annual rate of exceeding a given IM level. $G(EDP \mid IM)$ represents the complementary cumulative distribution function (CCDF) of EDP conditional to a given level of IM, i.e., $G(EDP \mid IM) = P[EDP \geq y \mid IM = x]$. $G(DM \mid EDP)$ and $G(DV \mid DM)$ are defined in a similar manner.

The key assumption of the whole procedure is the conditional independence of DV and DM from IM, of DV from EDP and IM. This implies that intermediate variables EDP and DM, used to relate IM to DV, are chosen so that the conditioning information is not "carried forward". It is to note that IM, EDP, DM and DV can potentially also be vectors (Yeo and Cornell, 2005).

All previous components are usually considered to be time-invariant; however, variation in time of seismic structural risk may involve all three components that form the performance-based earthquake engineering framework (Cornell and Krawinkler, 2000). This thesis focuses on the time-variant aspects that can involve both the hazard and the vulnerability assessment. In the following sections the traditional approaches used to evaluate the seismic hazard and the vulnerability are described. Hence, different cases where time-variant approaches may be suitable are presented.

1.2. Probabilistic Seismic Hazard Analysis

One of the most important ingredients of the PEER equation is the evaluation of the seismic hazard. Ever since probabilistic seismic hazard analysis was developed in the late 1960s, the modeling of earthquakes occurrence has drawn considerable interest from various investigators (Villani, 2010). Thus, recurrence models have evolved significantly since they were first introduced. The stochastic processes which are used to model the earthquake generating phenomenon are based on the assumption that the occurrence of an earthquake in a region is independent of subsequent and previous earthquakes in that region.

Hence, probabilistic seismic hazard analysis usually refers to homogeneous Poisson process (HPP) to probabilistically model earthquake occurrence. The latter is an independent- and stationary-increment (i.e., memory-less) model, which may be especially suitable when several (independent) sources contribute to the seismic threat for a site. This process has no memory of the past earthquakes, consequently, the occurrence of an event does not depend on how long it has been since the last event, that is, an event can occur at any time. The number of events, N_E, occurring in the time interval of interest, $(t, t+\Delta T)$, is Poisson distributed as in Equation (1.2), with mean $\nu_E \cdot \Delta T$, where ν_E is the rate of the process (constant and time independent).

$$P\left[N_E(t, t+\Delta T) = n\right] = P\left[N_E(\Delta T) = n\right] = \frac{(\nu_E \cdot \Delta T)^n}{n!} \cdot e^{-\nu_E \Delta T} \tag{1.2}$$

Starting from the previous equation, the interarrival times are exponentially distributed, Equation (1.3).

$$f_T(t) = \nu_E \cdot e^{-\nu_E \cdot t} \tag{1.3}$$

The memoryless properties of this model are also put into evidence by the hazard rate function, *h(t)*, defined as the ratio between the density function and the complementary cumulative distribution function of the interarrival times. It describes the probability of

an immediate event since no event had occurred ‘till that instant. For the Poisson process, the hazard rate function, is constant and equal to the average rate ν_E, Equation (1.4).

$$h(t) = \frac{f(t)}{1 - F(t)} = \nu_E \tag{1.4}$$

This means that the probability of occurrence of an earthquake in a future small increment of time, remains constant independently of the size and the time spent since the last event.

Under the hypothesis of a Poisson earthquake recurrence model, the annual rate of exceedance of an IM threshold, $\lambda_{im,E}$, is obtained from ν_E via Equation 1.5, where the term $P[IM > im \mid x, y]$, provided by a ground motion prediction equation (GMPE), represents the probability that the intensity threshold is exceeded given an earthquake of magnitude $M_E = x$, from which the site is separated by a distance $R_E = y$.

$$\lambda_{im,E} = \nu_E \cdot \int_{r_{E,\min}}^{r_{E,\max}} \int_{m_{E,\min}}^{m_{E,\max}} P[IM > im \mid x, y] \cdot f_{M_E,R_E}(x, y) \cdot dx \cdot dy \tag{1.5}$$

The term f_{M_E,R_E} is the joint probability density function (PDF) of magnitude and distance random variables (RVs). In the case of a single source, if these two RVs may be considered stochastically independent, f_{M_E} is often described by a Gutenberg-Richter (GR) relationship (Gutenberg and Richter, 1944), and f_{R_E} is obtained on the basis of the source-site geometrical configuration. The integral limits are the magnitudes bounding the GR relationship and the distances defining the domain of possible R_E values (e.g., Reiter, 1990).

1.3. History-dependency in seismic hazard

History-dependent processes may be more appropriate to consider the occurrence of earthquakes on individual faults, fault interactions or to consider that earthquakes are typically clustered both in space and time. Moreover, they are suitable to consider a time scale different from that of the long term, that is, to perform an aftershock probabilistic seismic hazard analysis (APSHA; Yeo and Cornell 2009a).
In the following, different cases where a time-variant approach is suitable are briefly reviewed.

1.3.1. Long-term seismic hazard

The recurrence models for temporal behavior of earthquakes can roughly be subdivided into two types of processes, available in literature.
The former, *renewal processes*, are usually employed to probabilistically model characteristic events, that is, when the fault tends to generate similar magnitude events (note however that HPP is a renewal process as well). Such stochastic models are defined as *renewal* as they assume that the system restarts as-new after the occurrence of each event. In these processes, interarrival times are independent and identically distributed (i.i.d.) random variables. Moreover, as no other RVs are considered, such a distribution completely characterizes the model.
In the seismic context, renewal processes may be used to describe a sequence of large magnitude events, probabilistically modeling the mechanism of strain accumulation and release. In other words, they follow the average trend of elastic-rebound theory (Reid, 1910), which suggests that large tectonic earthquakes recur when a threshold elastic strain is reached in the crust. Strain is then released during the event and slowly re-accumulated by steady tectonic forces with a strain rate until the next event (Matthews et al., 2002).
The second category of processes differs from the previous one as in this case a relationship between interarrival time and event magnitude which are both considered as RVs is included. The two main models are: the time-predictable (e.g., Anagnos and

Kiremidijan 1988) and the slip-predictable (e.g., Kiremidijan and Anagnos 1984). Further details about them are reported in chapter 2, where different history-dependent models are reviewed.

1.3.2. Aftershock probabilistic seismic hazard analysis

After an earthquake of large magnitude (referred to as the mainshock), many triggered events or aftershocks may occur. Aftershocks sequences cannot be represented by the homogeneous Poisson process since their rate appears to be dependent on the time, magnitude and location of the mainshock. For this reason a non-homogeneous Poisson process (NHPP) may be appropriate to probabilistically describe their occurrence. The importance of modeling aftershocks occurrence is related to the fact that aftershock ground motions may cause weakening and/or collapse of structures perhaps already damaged (but not yet repaired) by the mainshock. Moreover, aftershocks hazard is larger than mainshock hazard (computed trough a HPP) for many days after the occurrence of an event.

Recently, Yeo and Cornell (2009a) have developed aftershock-PSHA to express aftershock hazard similar to the mainshock hazard; i.e., in terms of probability of exceedance of a ground motion intensity measure threshold. This is useful in the post-mainshock emergency phase and for short-term risk management.

The main assumption for the aftershocks probabilistic seismic hazard analysis is that the aftershock occurrence rate cannot be considered time-invariant. In fact, after the occurrence of a mainshock, the rate is at its maximum and then decreases with the increasing elapsed time from the occurrence of the mainshock in accordance with the *modified Omori law*. In accordance with this law, the instantaneous aftershock rate per day is expressed as a function of $(t+c)^p$, where t is the number of elapsed days from the mainshock, while c and p are constant values for a particular aftershock sequence. The mean instantaneous daily rate of aftershocks with moment magnitude m, or larger, at time t, following a mainshock of moment magnitude m_E, can be calculated using Equation (1.6), where a and b are the Gutenberg-Richter relationship parameters.

$$\nu_{A|m_E}(t) = \left(10^{a+b\cdot(m_E-m_{\min})} - 10^{a}\right) \Big/ (t+c)^{p} \tag{1.6}$$

The expected number of aftershocks with magnitudes between $m_{\min}$ (a lower bound aftershock magnitude of engineering interest) and m_E in the time interval $[t, t+\Delta T_A]$ following a mainshock of magnitude m_m can be evaluated through Equation (1.7).

$$E\left[N_{A|m_E}(t, t+\Delta T_A)\right] = \\ = \int_{t}^{t+\Delta T_A} \nu_{A|m_E}(\tau)\cdot d\tau = \frac{10^{a+b\cdot(m_E-m_{\min})} - 10^{a}}{p-1} \cdot \left[(t+c)^{1-p} - (t+\Delta T_A + c)^{1-p}\right] \tag{1.7}$$

Since the daily rate of aftershocks is time-variant, a non-homogeneous Poisson process is used to model aftershocks occurrence, Equation (1.8).

$$P\left[N(t, t+\Delta T_A) = n\right] = \frac{\left[\int_{t}^{t+\Delta T_A} \nu_{A|m_E}(\tau)\cdot d\tau\right]^{n}}{n!} \cdot \exp\left[-\int_{t}^{t+\Delta T_A} \nu_{A|m_E}(\tau)\cdot d\tau\right] \tag{1.8}$$

NHPP requires a time-variant rate of exceeding site ground motion im in $[t, t+\Delta T_A]$ which can be computed, through Equation (1.9), in which $P[IM > im \mid m, r]$ is the probability that intensity threshold is exceeded given an aftershock of magnitude m and separated from the site of interest by a distance equal to r while f_{M_A, R_A} is the joint PDF of magnitude and source-to-site distance of the generic aftershock.

$$\lambda_{im, A|m_E}(t) = \nu_{A|m_E}(t) \cdot \int_{r_{A,\min}}^{r_{A,\max}} \int_{m_{\min}}^{m_E} P[IM > im \mid w, z] \cdot f_{M_A, R_A}(w, z) \cdot dw \cdot dz \tag{1.9}$$

1.3.3. Further time-variant aspects in seismic hazard analysis

The APSHA put into evidence one of the most important characteristics of earthquakes, that is, their tendency to cluster both in space and time.

In literature, there exist some models that account for the occurrence of the whole cluster, even though they usually refer to different time scales. Among the few spatio-temporal models present in literature, the Epidemic Type Aftershock Sequence (ETAS) model is one of the most studied and applied (Console et al. 2007; Zhuang et al. 2011; Zhuang et al., 2002).

Such a model was suggested by Ogata (1988). It assumes that each event produces events independently of the others. The probability distribution of the time until the occurrence of an earthquake is a function of the time spent since the last event and is independent of the magnitude. Instead, the probability distributions of location and magnitude of the triggered event are dependent on the magnitude and the location of the triggering one. The magnitudes of all the events, including background events and their offspring, are independent random variables drawn from the same probability distribution of density.

Boyd (2012), instead, incorporated foreshocks and aftershocks into time-independent probabilistic seismic-hazard analysis. The author assumes the mainshock and its dependents as a time-independent cluster, each cluster being temporally and spatially independent from any other. The cluster has a recurrence time of the mainshock and, by considering the earthquakes in the cluster as a union of events, dependent events have an opportunity to contribute to seismic ground motions and hazard. It is to note, however, that the author, to perform the seismic hazard analysis does not provide an analytical formulation, but generates multiple synthetic sets of foreshocks and aftershocks with which to do the clustering analysis.

Another aspect of the seismic hazard for which it should be suitable to use history-dependent models is the interaction among different faults. In fact, when an event occurs it provides a tectonic loading change in surrounding regions where the perturbation of the stress level may delay or move up the occurrence of an event. In literature, there are different stochastic models that permit to consider that the stress

release on a fault may change the stress level on another one causing a triggering mechanism. The first one is the *"linked" stress release model*, which is an extension of the simple stress release model proposed by Vere-Jones (1978). In such a model, the accumulated stress release of earthquakes that occurred in a region is considered and a specific parameter measures the fraction of stress transferred from a region to another one. The second model, provided by Console et al. (2010) considers that, given a segment of fault, the earthquakes in the surrounding regions may produce a change in the coseismic static permanent Coulomb stress (ΔCFF) that can delay or anticipate the occurrence of an event on that fault.

1.4. Seismic vulnerability

The vulnerability of a system may be affected by different phenomena of deterioration that lead the vulnerability to be history-dependent. In particular, some deterioration mechanism may increase the physical vulnerability of the system, improving the risk of structural failure. Two main sources of deterioration, which result to change in the mechanical characteristics of a structural system, are usually considered.

The first one has substantially continuous effects and is usually tied to environmental and operating conditions (e.g., aging). The aging process is often related to aggressive environment, which worsens mechanical features of structural elements. Aging, therefore, directly affects the static and dynamic response of the structures and may show an effect in increasing seismic structural fragility. Since the time-variant changes are random in nature, the safety evaluation of the existing structures can be conducted rationally within a probabilistic framework (Shinozuka, 1983), taking into account various sources of uncertainty with respect to the deterioration process. However, the behavior of material in time and under variable conditions is a complex and multidimensional problem.

The other source of deterioration has effects that are superposed occasionally to the first effects, and are usually related to external sudden actions, for example due to cumulative earthquake damage (e.g., Sanchez-Silva et al., 2011); thesis focuses on this last aspect.

Recent literature about life-cycle models for earthquake resistant structures considers that damage accumulation and failure are possibly due to subsequent shocks occurring during the time period of interest. This aspect is another important factor that may increase the risk of failure and that has to be treated in a time-variant probabilistic framework. Most of the seismic risk assessment models only consider the effect of mainshocks. This is also implicitly induced by common probabilistic seismic hazard analysis, which accounts for the exceedance of ground motion thresholds in compliance with memory-less Poisson processes. This is the reason why in the framework of Performance-Based Earthquake Engineering, structural fragility is usually assumed to be history-independent. Moreover, it is usually assumed that a structure, between two events, is repaired and this assumption justifies the fact that the risk assessment only considers intact structures. On the other hand, it is well known that earthquakes occur in clusters in which the mainshock represents only the principal event. Because there is a chance that also aftershocks worsen structural conditions, it may be appropriate to include this effect in the life-cycle assessment, also considering that the interval between subsequent shocks is insufficient to repair the structure (Yeo and Cornell, 2009b). Recently, stochastic processes of aftershock sequences and their effect on cumulative structural damage have been formalized. In the case only post-mainshock context is considered, the collapse risk is assumed caused by the occurrence of aftershocks and usually, in this framework, the state of structure is quantified in terms of discrete damage states (Luco et al., 2011). In this approach, the performance of the system at a certain time, is a combination of two main factors: (i) the initial damage state of the structure (which is not necessarily known) and (ii) the capacity of the damaged building to resist to future events. The increment of damage in each event is therefore state-dependent, that is, the response of the structure depends on the state the earthquake found the system.

An alternative approach based on the reduction of a parameter representing the seismic performance of the structure, or on the increase of a variable representing the damage accumulation over progressive cycles, is particularly interesting for life-cycle analysis.

One of the last developed models is that proposed by Iervolino et al. (2013a). This model is briefly reviewed as the basis of the stochastic modeling of structures

cumulating damage formalized in this thesis. The model assumes as damage index, a measure proxy for the dissipated hysteretic energy that allows to consider that damage increments in subsequent events are i.i.d. RVs, that is, the response of the structure to any specific earthquake is independent of its status prior to the shock. One of these measures is the *kinematic ductility*, μ, which is the maximum displacement demand when the yielding displacement is the unit and it is suitable for a *non-evolutionary* elastic-perfectly-plastic (EPP) single degree of freedom system system (SDoF). In particular, the degradation process is formulated as in Equation (1.10), where μ^* is the capacity at $t=0$, immediately after the mainshock of interest, and $D(t)$ is the cumulated damage due to all aftershocks, $N(t)$, occurring within *t*. Both $\Delta\mu_i$ (damage in one aftershock) and $N(t)$ are RVs.

$$\mu(t) = \mu^* - D(t) = \mu^* - \sum_{i=1}^{N(t)} \Delta\mu_i \tag{1.10}$$

Given this formulation, the probability the structure fails within time *t*, $P_f(t)$, is the probability that the structure passes the limit-state threshold, μ_{LS}, or the complement to one of reliability, $R(t)$, Equation (1.11). In fact, it is the probability the cumulated damage is larger than the difference between the initial value and the threshold, $\bar{\mu} = \mu^* - \mu_{LS}$.

$$P_f(t) = 1 - R(t) = P\left[\mu(t) \le \mu_{LS}\right] = P\left[D(t) \ge \mu^* - \mu_{LS}\right] = P\left[D(t) \ge \bar{\mu}\right] \tag{1.11}$$

In particular, using the total probability theorem, $P_f(t)$ may be computed from Equation (1.12), where $P\left[N(t)=k\right]$ may be calculated considering that the occurrence of aftershocks follows a NHPP, while $P\left[D(t) \ge \bar{\mu} \middle| N(t)=k\right]$, that is, the probability of cumulative damage exceeding the threshold conditional to number of

shocks may be easily computed if the distribution of the sum of damages can be expressed in a simple form.

$$P_f(t) = \sum_{k=1}^{+\infty} P\left[D(t) \geq \bar{\mu} \middle| N(t) = k \right] \cdot P\left[N(t) = k \right] \tag{1.12}$$

In particular, authors assuming that damage increments are described by a *gamma* distribution, which enjoys the reproductive property, obtain a closed-form solution for the probability of failure conditional to a given number of shocks.
However, it should be of interest to consider the aftershock contribute not only in the post mainshock context, but at the scale of the life of the structure, while Iervolino et al. (2013b) propose a similar model for the long term, it does not account for aftershocks. Therefore, in this thesis, a stochastic modeling of structures cumulating damage due to mainshock-aftershock seismic sequences has been developed to consider the effect of the whole cluster.

1.5. Outline of the Thesis

In **Chapter 2**, attention is focused on the long-term seismic hazard analysis evaluated using history-dependent models. Among the renewal processes, three different cases are considered: the Brownian Passage Time (BPT); a renewal process with Erlang (i.e., Gamma with integer shape parameter) interarrival time distribution; and finally, a model in which it is assumed that an inverted Gamma distribution represents the interarrival time.
The BPT model is chosen because very well known in the field; the second one because it allows to formulate the counting process of events in a closed-form; the third process, assumes that the stress rate accumulation is a random variable Gamma-distributed which lead to an inverted-Gamma interarrival time distribution.
Among processes that consider both interarrival time and magnitude as RVs, the time-predictable (e.g., Anagnos and Kiremidijan, 1988) and the slip-predictable (e.g., Kiremidijan and Anagnos 1984) are reviewed.

As an illustrative application, the Paganica fault (in central Italy) is considered to compute the seismic hazard, in terms of ground motion intensity measure, according to each of the models. Examples also include, as a benchmark, hazard when HPP is considered.

In **Chapter 3**, starting from the APSHA and following Boyd (2012), it is shown how it is possible to analytically combine results of PSHA and APSHA to get a probabilistic seismic hazard analysis for mainshock-aftershocks seismic sequences.
Considering a seismic cluster as the whole of mainshock and following aftershock sequence, it may be argued that the occurrence of clusters is probabilistically described by the same rate of the main event. It is built on the hypotheses of HPP occurrence of mainshocks, aftershock occurrence may be modelled via a non-homogeneous Poisson process with a rate, which depends on the magnitude of the triggering mainshock according to the model of Yeo and Cornell (2009a).
The combination of PSHA and APSHA is analytically discussed and, as an illustrative application, a generic seismogenic source is considered and the SPSHA expressed in terms of annual rate of exceedance of different IM-levels is finally computed.
Results of the illustrative application presented help to assess the increase in seismic hazard considering the probability of exceeding an acceleration threshold (e.g., that considered for design) also considering the contribution of aftershocks.

In **Chapter 4** a stochastic life-cycle damage accumulation model for earthquake resistant structures is developed, accounting for the effect of the whole cluster.
The developed compound point process assumes that damage increments are independent and identically distributed random variables and that the process regulating earthquake occurrence and seismic damage are mutually independent. It is shown that such a hypothesis may apply for simple, yet general, elastic-perfectly-plastic single degree of freedom systems, considering energy-based damage measures. According to the last hypothesis, earthquake's structural effects are i.i.d, that is, the structure, in an event, suffers damage that is independent of its state. These assumptions are also used to describe the cumulative damage in the single cluster,

where it is assumed that mainshock follows a homogeneous Poisson process while conditional aftershocks occurrence follows a non-homogeneous Poisson process, according to APSHA. Moreover, the model also considers that not all earthquakes are damaging; in fact, assuming that earthquake magnitude follows a Gutenberg-Richter relationship, not all events are strong enough to damage the structure.
An illustrative application referring to an EPP-SDoF structure is considered to compute the structural lifetime distribution. It is evaluated when the gamma and inverse Gaussian distributions (considering both the exact and approximated solution) are adopted to approximate the damage increment in one cluster.
The life-cycle assessment is also compared with the case damaging aftershock effect is ignored. Starting from the closed-form solutions, which provide the absolute (i.e., aprioristic) probability that a new structure fails in a time interval of interest, conditional failure probabilities, which account for information possibly available at the epoch of the evaluation, have been calculated.

In **Chapter 5**, the general outcomes deriving from the developing and the application of the proposed procedures are, finally, discussed.

References

Anagnos T, and Kiremidjian AS (1988). A review of earthquake occurrence models for seismic hazard analysis. *Probabilistic Engineering Mechanics* 3(1): 3-11.

Boyd OS (2012). Including foreshocks and aftershocks in time-independent probabilistic seismic hazard Analyses. *B. Seism. Soc. Am*. 102(3): 909-917.

Console R, Murru M, Catalli F and Falcone G (2007). Real time forecasts through an earthquake clustering model constrained by the rate-and-state constitutive law: comparison with a purely stochastic ETAS model. *Seismological Research Letters*, 78, 49–56. 3, 15

Console R, Murru M and Falcone G (2010). Perturbation of earthquake probability for interacting faults by static Coulomb stress changes. *Journal of Seismology* 14: 67-77. doi:10.1007/s10950-008-9149-4

Cornell CA, Krawinkler H (2000). Progress and challenges in seismic performance assessment. *Peer Center Newletter*, 3(2).

Iervolino I, Giorgio M, Chioccarelli E (2013). Gamma degradation models for earthquake resistant structures. *Struct. Saf*. 45: 48–58.

Gutenberg R, Richter CF (1944). Frequency of earthquakes in California, *Bulletin of the Seismological Society of America*, 34(4), 185-188.

Kiremidjian AS and Anagnos T (1984). Stochastic slip-predictable model for earthquake occurrences. *Bulletin of the Seismological Society of America* 74(2): 739-755.

Luco N, Gerstenberger MC, Uma SR, Ryu H, Liel AB and Raghunandan M (2011). A methodology for post-mainshock probabilistic assessment of building collapse risk. *Ninth Pacific Conference on Earthquake Engineering, Auckland, New Zealand.*

Matthews VM, Ellsworth LW and Reasenberg AP (2002). A Brownian model for recurrent earthquakes. *Bulletin of the Seismological Society of America* 92(6): 2233-2250.

McGuire RK (2004). Seismic Hazard and Risk Analysis, Earthquake Engineering

Research Institute, MNO-10, Oakland, California, 178 pp.

Ogata Y (1988). Statistical models for earthquake occurrences and residual analysis for point processes. J. *Am. Stat. Assoc*., 83, 9 – 27. 3

Reasenberg PA and Jones LM (1989). Earthquake hazard after a mainshock in California. *Science* 243: 1173-1176.

Reid HF (1910). The Mechanics of the Earthquake, The California Earthquake of April 18, 1906, Report of the State Investigation Commission, Vol.2, Carnegie Institution of Washington, Washington, D.C.

Reiter L (1990). Earthquake hazard analysis: issues and insights, Columbia University Press, New York.

Sanchez-Silva M, Klutke G-A, Rosowsky DV (2011). Life-cycle performance of structures subject to multiple deterioration mechanisms. *Struct. Saf.*, 33(3), 206–217.

Shinozuka M (1983). Basic analysis of structural safety, *J. Struct. Eng*. (ASCE), 109 (3), 721–740.

Shome N and Cornell CA (2006). Probabilistic seismic demand analysis for a vector of parameters. 8th US National Conference on Earthquake Engineering, San Francisco, CA.

Vamvatsikos D and Cornell CA (2002). Incremental Dynamic Analysis. *Earthquake Engineering & Structural Dynamics,* 31(3), p. 491-514.

Vere-Jones D (1978). Earthquake prediction: A statistician's view, *J. Phys. Earth*, 26, 129–146.

Villani M (2010). High resolution SHA in the vicinity of earthquake sources. PhD thesis.

Yeo GL and Cornell CA (2005). Stochastic characterization and decision bases under time-dependent aftershock risk in performance-based earthquake engineering. *PEER Report 2005/13, Department of Civil and Environmental Engineering, Stanford University, Stanford, CA.*

Yeo GL and Cornell CA (2009a) A probabilistic framework for quantification of aftershock ground-motion hazard in California: Methodology and parametric study. Earthquake Eng. Struct. Dyn. 38: 45-60.

Yeo GL and Cornell CA (2009b). Building life-cycle cost analysis due to mainshock and aftershock occurrences. *Struct. Saf.*, 31(5), 396–408.

Zhuang J, Ogata Y and Vere-Jones D (2002). Stochastic declustering of space-time earthquake occurrences. *J. Am. Stat. Assoc*., 97:369-80.

Zhuang J, Werner MJ, Hainzl S, Harte D and Zhou S (2011). Basic models of seismicity: spatiotemporal models, Community Online Resource for Statistical Seismicity Analysis, doi: 10.5078/corssa-07487583. Available at http://www.corssa.org.

Chapter 2 - MODELS AND ISSUES IN HISTORY-DEPENDENT MAINSHOCK HAZARD

This chapter is derived from the following paper:

Polidoro B., Iervolino I., Chioccarelli E., Giorgio M. (2013). Models and issues in time-dependent mainshock hazard. ICOSSAR, 11th International Conference on Structural Safety & Reliability 16-20 June, Columbia University, New York.

2.1. Introduction

Probabilistic seismic hazard analysis (PSHA; e.g., McGuire, 2004) usually refers to homogeneous Poisson process (HPP) to probabilistically model earthquake occurrence. The latter is an independent- and stationary-increment (i.e., memory-less) model, which may prove suitable when several (independent) sources contribute to the seismic threat for a site. However, when a single fault is of concern and/or the time scale is different from that of the long term, other models may be more appropriate to probabilistically describe the earthquakes occurrence process.

The long-term mainshock occurrence is considered in this paper, neglecting other cases as the short-term aftershock sequence modeling (e.g., Yeo and Cornell, 2005) or the multi-scale operational forecasting (e.g., Jordan et al., 2011). In fact, the study focuses on two types of history-dependent models. The first category is that of renewal processes, which applies when characteristic earthquakes are of concern, that herein is when the considered source may produce a specific magnitude. The second type, which can be formalized on the basis of the theory of Markov renewal processes, enables, as an additional feature, modeling of correlation between magnitude and interarrival time; e.g., Anagnos and Kiremidijan (1988); Cornell and Winterstein (1988).

The study is structured such that assumptions common to all the considered models are

presented first. Then, modeling of the random variables (RVs) involved in each of them, is reviewed. Moreover, an illustrative application is set-up with respect to evaluate the conditional probability of exceedance of a ground motion intensity measure (IM) value for a site of interest, and in a given time-frame.
To this aim, the Paganica fault (in central Italy; believed to be the source of the 2009 L'Aquila earthquake) and a site close to it are considered. This allows to compute, for each history-dependent model, the probability of observing one event in the time interval of interest, and the probability of exceedance of an IM-level, as a function of the time elapsed since the last earthquake.

2.2. Renewal processes for earthquake occurrence

A renewal process (RP) is, by definition, a sequence of independent and identically distributed (i.i.d.) non negative RVs (whose distribution completely characterizes the model). In the considered application the RV of interest is the time between successive occurrences of earthquakes (i.e., interarrival time, T).
In the seismic context, RPs appear suitable to describe a sequence of similar and large magnitude events on a specific seismic source in the context of the elastic-rebound theory (Reid, 1910), which suggests that large tectonic earthquakes may recur at the onset of large elastic strain in the crust. Strain will then re-accumulate slowly by steady tectonic forcing until the next event.
In fact, in all RPs it is assumed that the system (i.e., the earthquake source) restarts as-new after the occurrence of each earthquake. In this sense, they appear suitable to model occurrence of characteristic earthquakes, that is sources that tend to produce specific-magnitude events.
The renewal processes considered are: (1) an inverse Gaussian RP, related to the Brownian relaxation oscillator model, (2) an Erlang RP, featuring an analytically tractable counting process; (3) and finally an inverse gamma RP, related to a model in which load increases deterministically over time with random loading rate.

2.2.1. Inverse Gaussian

This RP relates to the Brownian relaxation oscillator model. According to this model, load state, $X(t)$, increases gradually over time until it reaches an earthquake-triggering threshold. The model assumes that earthquake occurrence instantaneously relaxes back the system to some ground level. Load state process is modeled through a process with independent and stationary Gaussian-distributed increments, as in Equation (2.1) and sketched in Figure 2.1.

In the equation, $\dot{u}$ is the rate, $W(t)$ is the standard Brownian motion, which has stationary and independent Gaussian increments, and σ is a scaling factor that models process variance (Matthews et al., 2002). The deterministic (linearly increasing) part of the process, takes into account the constant-rate average loading, the random part represents contributions of all other factors affecting the eventual rupture of the considered source.

$$X(t) = \dot{u} \cdot t + \sigma \cdot W(t) \tag{2.1}$$

It is possible to show that, according to the above assumptions, the probability density function (PDF) of interarrival time, $f_T(t)$, follows an inverse Gaussian distribution, Equation (2.2). This PDF, which is also called the Brownian passage time (BPT) distribution, is entirely described by two parameters: the mean recurrence time (μ, the mean interarrival time, also referred to as the return period, Tr) and the coefficient of variation, or aperiodicity, of interarrival time (α). The return period is in relation with the load rate $(\dot{u})$ and the threshold $(\bar{u})$.

$$\begin{cases} f_T(t) = \sqrt{\dfrac{\mu}{2 \cdot \pi \cdot \alpha^2 \cdot t^3}} \cdot e^{-\frac{(t-\mu)^2}{2 \cdot \mu \cdot \alpha^2 \cdot t}} \\ \mu = \dfrac{\bar{u}}{\dot{u}} \end{cases} \tag{2.2}$$

The mean interarrival time or its reciprocal, the mean rate of occurrence, is the parameter of first order interest, that is the best-estimate of frequency at which events occur. The aperiodicity is a measure of irregularity in the event sequence, that is, a deterministic sequence features $\alpha = 0$.

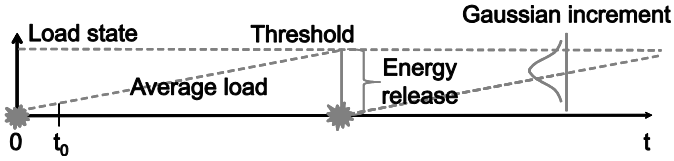

Figure 2.1. Sketch of source load modeling in the BPT model.

2.2.2. Erlang-distributed interarrival time RP

To define this process, an Erlang distribution (i.e., a gamma PDF with, k, as the integer shape parameter and λ as the scale parameter) for the interarrival time is considered. The interarrival time distribution is given in Equation (2.3), where Γ is the gamma function. This PDF has a flexible shape that can easily characterize any data-derived distribution (Takahashi et al., 2004).

Note that the mean and the coefficient of variation (CoV) in this case are given by k/λ and $1/\sqrt{k}$, respectively. These may be put in relation with the return period and the aperiodicity of the BPT model.

$$\begin{cases} f_T(t) = \dfrac{\lambda \cdot (\lambda \cdot t)^{k-1}}{\Gamma(k)} \cdot \mathrm{e}^{-\lambda \cdot t} \\ E[T] = \dfrac{k}{\lambda} \\ CoV[T] = \dfrac{1}{\sqrt{k}} \end{cases} \tag{2.3}$$

One of the main advantages of this process is that it allows a closed-form solution for the probability of occurrence of at least one event in time interval (t_0, t), given that the

last earthquake occurred at $t=0$, Equation (2.4). In the equation, t_0 is the time of the probabilistic assessment, and $N(t)$ is the function counting events in $(0,t)$.

$$P\left[N(t)\geq 1 \mid N(t_0)=0\right]=1-P\left[N(t)=0 \mid N(t_0)=0\right]=1-\frac{\sum_{i=0}^{k-1}\frac{(\lambda\cdot t)^i}{i!}\cdot e^{-\lambda\cdot t}}{\sum_{i=0}^{k-1}\frac{(\lambda\cdot t_0)^i}{i!}\cdot e^{-\lambda\cdot t_0}} \tag{2.4}$$

If the probability of having exactly one event is computed as in Equation (2.5), it is possible to evaluate how likely is that more than one earthquake occurs in the time-frame of interest as a function of the time elapsed since the last event, Figure 2.2.
This allows to understand that if the interval of interest is small with respect to the average recurrence time, as it usually happens for seismic risk analysis of engineering interest, the probability of having more than one event is very close to the probability of one event.
In other words, it is unlikely that more than one earthquake occurs in a small time interval. This result will be helpful in probabilistic seismic hazard analysis discussed in Section 2.4.

$$P\left[N(t)=1 \mid N(t_0)=0\right]=$$
$$=\frac{1}{\sum_{i=0}^{k-1}\frac{(\lambda\cdot t_0)^i}{i!}\cdot e^{-\lambda\cdot t_0}}\cdot\sum_{i=0}^{k-1}\left[\frac{(\lambda\cdot t_0)^i}{i!}\cdot e^{-\lambda\cdot t_0}\times\sum_{j=k-i}^{2\cdot k-i-1}\frac{\left[\lambda\cdot(t-t_0)\right]^j}{j!}\cdot e^{-\lambda\cdot(t-t_0)}\right] \tag{2.5}$$

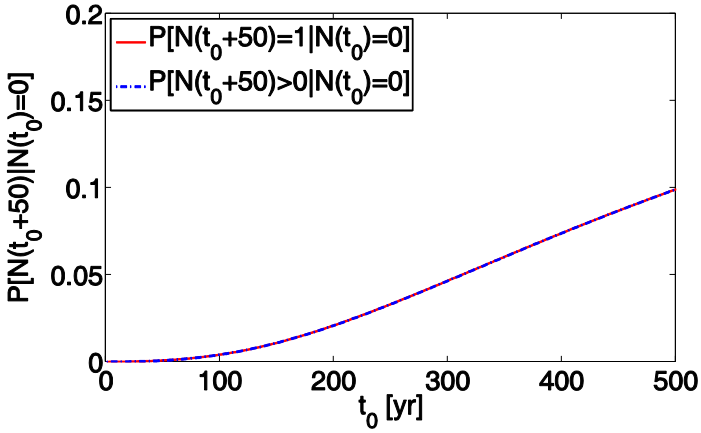

Figure 2.2. Comparison between the probability of observing exactly one event, and at least one event, for the renewal process with gamma interarrival time distribution in a 50 yr time frame, as a function of the time elapsed since the last earthquake.

2.2.3. Inverse-Gamma-distributed interarrival time RP

This RP relates to a (simple) model, which assumes that the load on the fault increases linearly and deterministically over time, with a rate that varies randomly from event to event.

Rate is modeled as a gamma-distributed random variable. The earthquake occurs once a threshold is reached. Then, the system resets itself until the next event, Figure 2.3.

It is possible to show that these hypotheses lead to a renewal process characterized by an inverse-gamma-distributed (IG) interarrival time (Pandey and van Noortwijk, 2004). The latter is given in Equation (2.6), where γ and β are the shape and scale parameters, respectively. In the equation the mean and variance of the RV are also given as a function of the parameters.

$$\begin{cases} f_T(t) = \dfrac{\beta^\gamma}{\Gamma(\gamma)} \cdot \left(\dfrac{1}{t}\right)^{\gamma+1} \cdot e^{-\frac{\beta}{t}} \\ E[T] = \dfrac{\beta}{\gamma - 1}, & \gamma > 1 \\ Var[T] = \dfrac{\beta^2}{(\gamma-1)^2 \cdot (\gamma-2)}, & \gamma > 2 \end{cases} \tag{2.6}$$

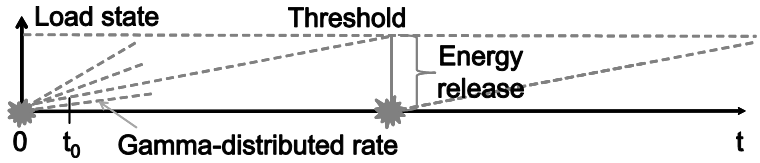

Figure 2.3. Representation of loading in the renewal process with Gamma-distributed load rate.

2.2.4. Homogeneous Poisson process

It is to note that the HPP model may also be seen as a renewal process with exponential interarrival time, Equation (2.7), with mean and standard deviation equal to μ and Poisson distribution for the increments of the associated counting process, Equation (2.8). The latter has independent and stationary increments that render the process memory-less.

$$f_T(t) = \frac{1}{\mu} \cdot e^{-\frac{t}{\mu}} \tag{2.7}$$

$$P\left[N(t) = n \mid N(t_0) = 0\right] = P\left[N(t - t_0) = n\right] = \frac{\left[(t - t_0)/\mu\right]^n}{n!} \cdot e^{-(t-t_0)/\mu} \tag{2.8}$$

2.3. Markov renewal processes

The models reviewed in this section are of particular earthquake engineering interest, as they allow modeling the relationship between the time and the magnitude of the

earthquake (i.e., correlation between these RVs). Two simple examples of these Markov renewal processes (MRPs) are herein considered: the *time-predictable* and the *slip-predictable* models.

2.3.1. Slip Predictable model

The slip-predictable model (SPM), similarly to those in Section 2.2, may represent the case in which the stress accumulates starting from some initial level for a random period of time until an earthquake occurs (Kiremidjian and Anagnos, 1984).
Interarrival times are modeled as Weibull independent and identically distributed RVs. The PDF, along with mean and variance, are given in Equation (2.9), where b and $1/a$ are the shape and scale parameters, respectively.

$$\begin{cases} f_T(t) = (a \cdot b) \cdot (a \cdot t)^{b-1} \cdot e^{-(a \cdot t)^b} \\ E[T] = \frac{1}{a} \cdot \Gamma\left(1 + b^{-1}\right) \\ Var[T] = \left(\frac{1}{a}\right)^2 \cdot \left[\Gamma\left(1 + 2 \cdot b^{-1}\right) - \Gamma^2\left(1 + b^{-1}\right)\right] \end{cases} \tag{2.9}$$

In particular, in SPM, the magnitude (M) of the next event depends on the time since the last earthquake (Figure 2.4) via the functional relationship, $m = g(t)$, taken deterministic herein. Hence, assuming that the next event will occur in the interval (t_0, t), the PDF of M depends on t_0 and t as in Equation (2.10).

This will be more clearly addressed in the application discussed in Section 2.4; it is to note here, however, that the SPM implies to not assume a fixed threshold for earthquake-related energy release.

$$f_{M|N(t_0)=0\cap N(t)=1}(m)=\begin{cases}\dfrac{f_T\left(g^{-1}(m)\right)}{\int_{t_0}^{t} f_T(z)\cdot dz}\cdot\dfrac{dg^{-1}(m)}{dm}, & m\in\left]g(t_0),g(t)\right] \\ 0, & m\notin\left]g(t_0),g(t)\right]\end{cases} \tag{2.10}$$

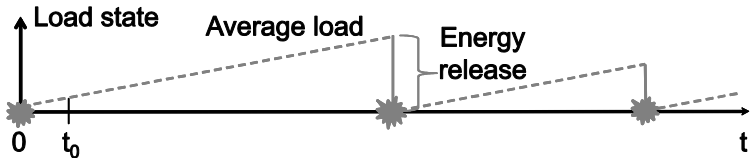

Figure 2.4. Loading and energy release in the SPM.

2.3.2. Time Predictable model

The time-predictable model (TPM) assumes that the time of occurrence of the next earthquake depends on the size and the time of occurrence of the last event (Anagnos and Kiremidjian, 1984). In fact, the larger the last earthquake, the longer is, on average, the time to the next event.

This hypothesis is different from the slip-predictable assumption, which implies that the size of the preceding event does not affect the occurrence time of the next earthquake.

TPM may represent the stress buildup until a threshold at which an earthquake occurs and a random part of the accumulated energy is released (Figure 2.5).

The magnitudes of events are assumed to be independent and identically distributed random variables.

On the other hand, the interarrival times are Weibull-distributed RVs, conditional on the size of the last earthquake, Equation (2.11).

The PDF is the same as in Equation (2.9), except that its parameters depend on the magnitude, M_0, of the last event or, in other words, on time that is needed to accumulate sufficient stress to reach again the threshold.

$$f_{T|M_0}(t)=a_m\cdot b_m\cdot(a_m\cdot t)^{b_m-1}\cdot e^{-(a_m\cdot t)^{b_m}} \tag{2.11}$$

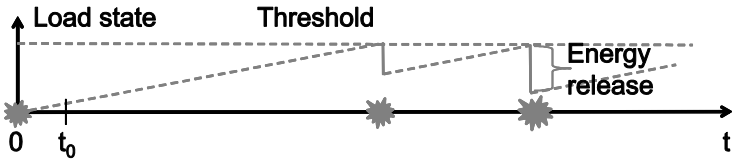

Figure 2.5. Loading and energy release in the TPM.

2.4. Probabilistic seismic hazard analysis in the case of hystory-dependent earthquake occurrence process

Considering each of the models above, the probability that the ground motion intensity measure exceeds a certain threshold, at least once in the next $t-t_0$ years (with $t>t_0$) given t_0 years passed since the last event, indicated as $P\left[IM>im \mid N(t_0)=0\right]$ for simplicity, can be written as in Equation (2.12). In the equation, the term $P\left[IM>im \mid m,r^*\right]$ represents the probability that intensity threshold is exceeded given an earthquake of magnitude *m* on the considered source. The latter is assumed to be separated from the site of interest by a distance equal to *R*; in the equation a fixed *R* value, *r**, is considered. This probability may be computed via ground motion prediction equations, or GMPEs.

$$
\begin{aligned}
&P\left[IM>im \mid N(t_0)=0\right]=\sum_{n=1}^{+\infty}P\left[IM>im \mid N(t_0)=0\cap N(t)=n\right]\times \\
&\times P\left[N(t)=n \mid N(t_0)=0\right]= \\
&\approx P\left[IM>im \mid N(t_0)=0\cap N(t)=1\right]\times P\left[N(t)=1 \mid N(t_0)=0\right]= \\
&\approx P\left[IM>im \mid N(t_0)=0\cap N(t)=1\right]\times P\left[N(t)\geq 1 \mid N(t_0)=0\right]= \\
&=P\left[IM>im \mid N(t_0)=0\cap N(t)=1\right]\times\left\{1-P\left[N(t)=0 \mid N(t_0)=0\right]\right\}= \\
&=\left\{1-P\left[N(t)=0 \mid N(t_0)=0\right]\right\}\times \\
&\times\int_m P\left[IM>im \mid m,r^*\right]\cdot f_{M\mid N(t_0)=0\cap N(t)=1}(m)\cdot dm
\end{aligned}
\tag{2.12}
$$

It is to note that Equation (2.12) avails of some approximations allowed by results of Section 2.2. It was found that in most of the cases of engineering interest, the interval of concern is much smaller than the return period of the characteristic event. Therefore, the probability in question can be computed considering only one term. Furthermore, the probability of occurrence of one event is about equal to that of at least one event (see Figure 2.2), which is relatively easy to compute.

2.5. Illustrative application

Hazard, in terms of peak ground acceleration (PGA), was computed according to the all reviewed models, considering the Paganica fault (central Italy) as a case-study (Figure 2.6). Hazard, here, is conditional on the time elapsed since the last event and its magnitude. Indeed, this kind of comparison is expected to highlight main differences among the reviewed models.

Models are calibrated so that they can be considered homogeneous only in terms of return period of an event of about M 6.3. Hence, more than on specific values of hazard, attention will be put on their trends.

In the case of BPT-, ERP-, and IG-RP, parameters of the interarrival time distributions were calibrated so that *Tr* is equal to 750 yr and the coefficient of variation is 0.43, which, according to Pace et al. (2006), characterize M 6.3 events on the Paganica fault. For the HPP the magnitude distribution was taken as a truncated exponential defined in the $[5.8, 6.8]$ interval as in Equation (2.13), while the rate of occurrence of HPP-described earthquakes was assumed to be 1/750 event/yr, Figure 2.7.

$$f_M(m) = \frac{2.49 \cdot e^{-2.49 \cdot (m - 5.8)}}{1 - e^{-2.49 \cdot (6.8 - 5.8)}} \tag{2.13}$$

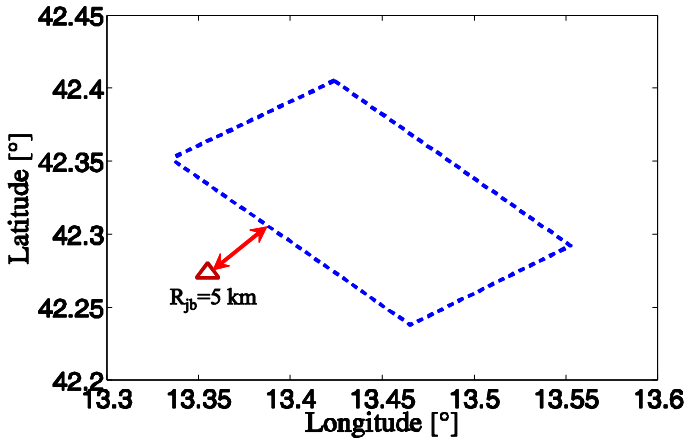

Figure 2.6. Source-site scheme.

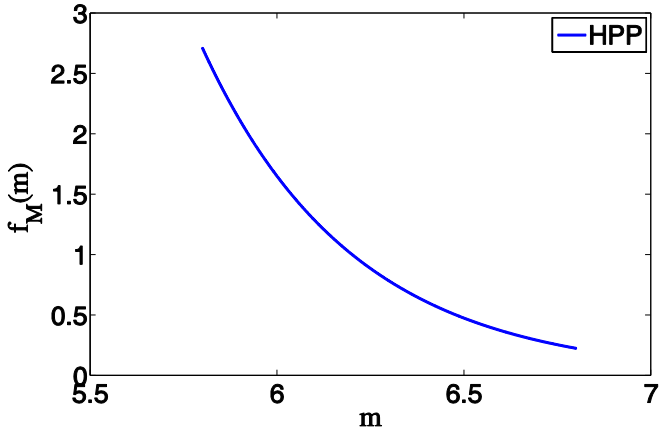

Figure 2.7. Exponential magnitude distribution for the HPP process on the fault.

For TPM, it was assumed that the last earthquake was a $M_0 = 6.3$ event, while M of the next characteristic event was considered to follow a truncated Gaussian distribution in the interval $[5.8, 6.8]$, that is, the mean value is set equal to 6.3, while a standard deviation equal to 0.1667 is adopted.

Finally, for SPM, all magnitudes were considered to be related to time of occurrence via Equation (2.14). A plot of the relationship is given in Figure 2.8.

$$t = 0.039 \cdot 10^{0.68 \cdot m} \tag{2.14}$$

The interarrival time distribution was calibrated in such a way that the mean of the interarrival time is equal to 750 yr and CoV is still 0.43.
This leads to the same parameters of the TPM interarrival time PDF; however, it is to underline that the return period of a M 6.3 event does not result in exactly 750 yr for this SPM, yet it is close to it. Indeed, even if 750 yr is the expected time to the next event, which can virtually be of any magnitude, such an event, by virtue of the time-magnitude relationship adopted, will be larger than M 5.8 with 0.91 probability.

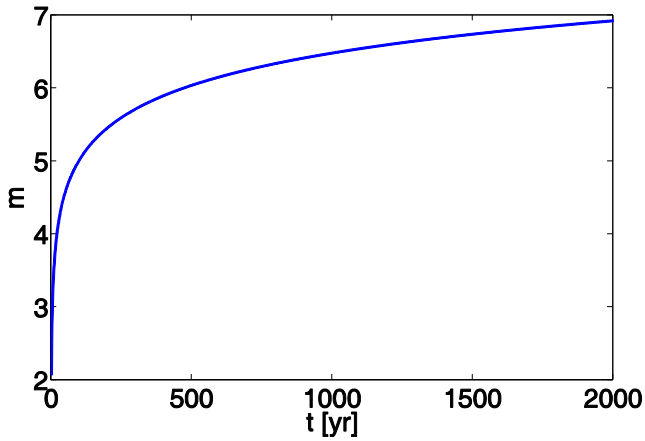

Figure 2.8. Time-magnitude relationship assumed.

In Table 1.1, the resulting parameters are given for all the models; note that in the Erlang case the mean value ant the CoV are slightly different because of the integer shape parameter.
Figure 2.9 shows the PDFs (that in this section are all indicated as $f_T(t)$, also in the case of TPM) computed via these values.

Table 1.1. Parameters of time to next event PDFs.

Model	Distribution Parameters		Tr [yr]	CoV
BPT	$\mu = 750$	$\alpha = 0.43$	750	0.43
Erlang	$k = 5$	$\lambda = 0.0072$	693	0.45
IG	$\gamma = 7.3$	$\beta = 4725$	750	0.43
SPM	$a = 0.00118$	$b = 2.5$	752	0.43
TPM	$a_{6.3} = 0.00118$	$b_{6.3} = 2.5$	752	0.43

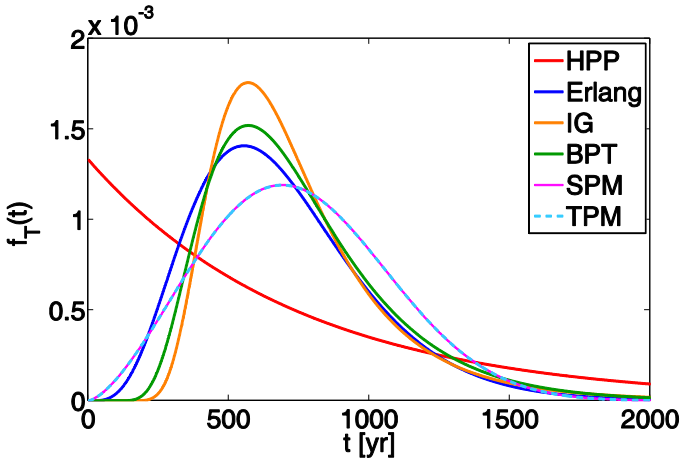

Figure 2.9. PDFs of interarrival time according to the considered processes.

2.6. Results and discussion

Figure 2.10 shows the probability of at least one event in a 50 yr time interval, calculated adopting $f_T(t)$ defined in Table 1.1.

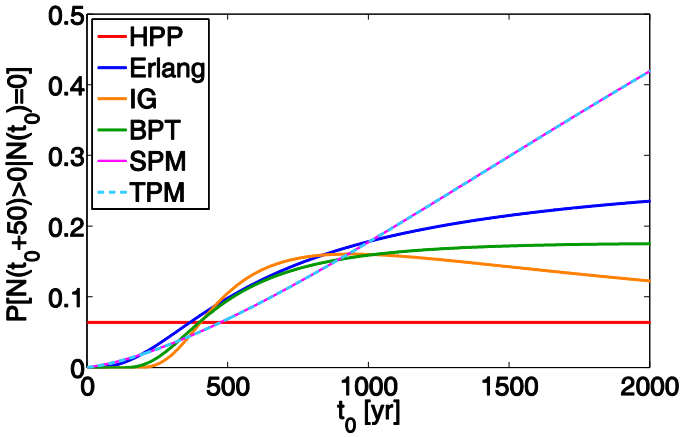

Figure 2.10. Probability of at least one event in 50 years as a function of the time since the last earthquake.

Trend observed in figure strictly depends on the shape of the hazard-rate function, Equation (2.15), which gives the instantaneous probability of an event occurrence given that no event had occurred until *t*.

$$h(t) = \frac{f_T(t)}{1 - F_T(t)} \tag{2.15}$$

It is noteworthy that, for some processes, after a certain time spent since the last earthquake, probability computed in figure tends to decrease. This depends on the fact that the hazard-rate function, associated to some of the considered $f_T(t)$, has a non-monotonic trend. In fact, as shown in Figure 2.11, BPT and IG models may have a non-monotonic hazard-rate functions that increase after the last earthquake, then decrease eventually (Matthews et al., 2002; Glen, 2011). Erlang RP with shape

parameter $k>1$ has a (bounded) increasing hazard-rate. Finally, SPM and TPM, with shape parameter of the Weibull distribution $b>1$, feature a diverging hazard-rate (Matthews et al., 2002). HPP has a constant hazard rate which is 1/750.
To compute seismic hazard expressed in terms of probability of exceedance of an IM-value in 50 yr, the approximation in Equation (2.12), whose suitability was shown for the Erlang renewal model, was assumed for all the other processes because of the similarity of the PDFs of the time to the next event (Figure 2.9).

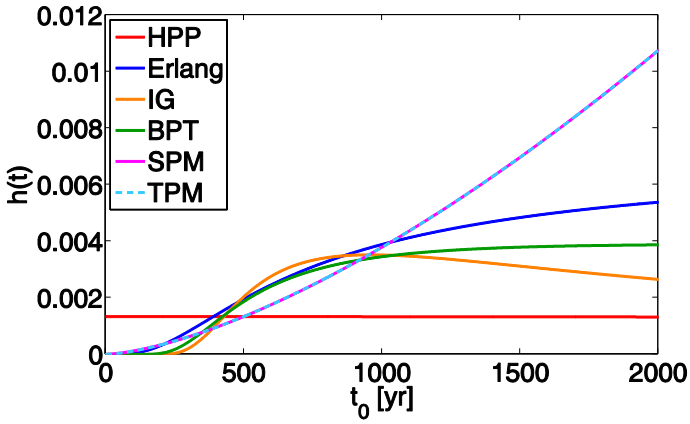

Figure 2.11. Hazard rate function for the different models.

To evaluate the $P\left[IM>im\,|\,m,r^{*}\right]$ term, the Sabetta and Pugliese (1996) GMPE was considered. The site was set at fixed Rjb distance (Joyner and Boore, 1981) equal to 5 Km (Figure 2.6).
In Figure 2.12 the probability that the PGA exceeds a certain threshold is plotted versus the time passed since the last event. The IM-threshold was assumed, as an example, equal to 0.447g. It is the median PGA given M 6.3 and r* = 5 km for shallow alluvium site according to the considered GMPE.
All history-dependent models, especially RPs, provide similar results for a time spent since the last earthquake of about one half of the return period of the event. Conversely, probabilities start to be increasingly different as t_0 gets significantly large.

This may render critical the selection of which one of the models to choose for a specific fault when the last known event is not recent.
The non-monotonic hazard-rate function of some of them also shows up in the results given in Figure 2.12, which indicates that the probability of exceedance of IM may decrease after a certain time since the last event, a behavior that may not be easy to justify.

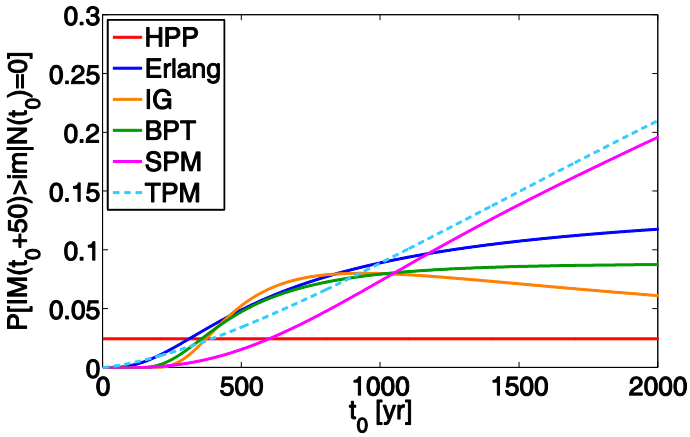

Figure 2.12. Hazard for PGA = 0.447 g.

2.7. Conclusions

The memory-less homogeneous Poisson process, where interarrival times are independent and identically distributed exponential random variables, is often used in hazard assessment for engineering seismic risk analysis. However, when a single fault is of concern and/or the time scale is different from that of the long term, history-dependent processes may be considered. In this paper, models for mainshock occurrence on an individual source, were reviewed with working examples. The models considered refer to the renewal, and Markov renewal point processes.
The Paganica fault (in central Italy) was considered to compute both the probability of occurrence of one event in the time interval of interest, as well as the seismic hazard,

expressed in terms of (conditional) probability of exceedance of an intensity value in a given time-frame.

The magnitude is considered to be that of characteristic events, that is when the considered source generates almost fixed-magnitude earthquakes. To homogenize the models, these were calibrated to have mean and variance of time to next event distributions as similar as possible.

Considering the time intervals of common engineering interest, it was assumed that the probability of more than one event is negligible (showed for the Erlang renewal process), simplifying hazard calculations.

It was also observed that because of the hazard-rate function, some processes show a decreasing probability of occurrence after a certain time has passed since the last event. This appears not to be the result of explicit representation of actual earthquake physics, while rather a collateral effect of the mathematics of the assumed models.

Engineering hazard analysis shows that history-dependent models have a similar trend, especially renewal processes, until a time of about a half of the mean return period of the event, and that the results from all models tend to relatively diverge as the elapsed time since the last event increases.

This means that the longer is the time spent since the last known earthquake on the source, the more critical is the selection of the process which is considered to be appropriate to represent earthquake occurrence.

References

Anagnos T and Kiremidjian AS (1984). Stochastic time-predictable model for earthquake occurrences. *Bulletin of the Seismological Society of America* 74(6): 2593-2611.

Anagnos T and Kiremidjian AS (1988). A review of earthquake occurrence models for seismic hazard analysis. *Probabilistic Engineering Mechanics* 3(1): 3-11.

Cornell CA and Winterstein SR (1988). Temporal and magnitude dependence in earthquake recurrence models. *Bulletin of the Seismological Society of America* 78(4): 1522-1537.

Glen AG (2011). On the Inverse Gamma as a Survival Distribution. *Journal of Quality technology* 43(2): 158-166.

Joyner WB and Boore DM (1981). Peak horizontal acceleration and velocity from strong motion records including records from the 1979 Imperial Valley, California, earthquake. *Bulletin of the Seismological Society of America* 71:2011-38.

Jordan T, Chen Y, Gasparini P, Madariaga R, Main I, Marzocchi W, Papadopoulos G, Sobolev G, Yamaoka K and Zschau J (2011). *Operational earthquake forecasting. State of Knowledge and Guidelines for Utilization.* Annals of Geophysics 54(4): 319-384.

Kiremidjian AS and Anagnos T (1984). Stochastic slip-predictable model for earthquake occurrences. *Bulletin of the Seismological Society of America* 74(2): 739-755.

Matthews VM, Ellsworth LW and Reasenberg AP (2002). A Brownian model for recurrent earthquakes. *Bulletin of the Seismological Society of America* 92(6): 2233-2250.

McGuire RK (2004). Seismic Hazard and Risk Analysis, *Earthquake Engineering Research Institute*, MNO-10, Oakland, California, 178 pp.

Pace B, Peruzza L, Lavecchia G and Boncio P (2006). Layered seismogenetic source model and probabilistic seismic-hazard analyses in central Italy. *Bulletin of the Seismological Society of America* 96(1): 107-132.

Pandey MD and van Noortwijk JM (2004). Gamma process model for time-dependent

structural reliability analysis. In E. Watanabe, D. M. Frangopol, and T. Utsonomiya, editors. Bridge Maintenance, Safety, Management and Cost, Proceedings of the Second International Conference on Bridge Maintenance, Safety and Management (IABMAS), Kyoto, Japan, Taylor & Francis Group, London.

Reid HF (1910). *The Mechanics of the Earthquake, The California Earthquake of April 18, 1906*, Report of the State Investigation Commission, Vol.2, Carnegie Institution of Washington, Washington, D.C.

Sabetta F and Pugliese A (1996). Estimation of response spectra and simulation of nonstationarity earthquake ground motion, *Bulletin of the Seismological Society of America* 86: 337–352.

Takahashi Y, Der Kiureghian A and Ang H-S A (2004). Life-cycle cost analysis based on a renewal model of earthquake occurrences. *Earthquake Engineering Structural Dynamics* 33: 859-880.

Yeo GL and Cornell CA (2005). *Stochastic Characterization and Decision Bases under Time-Dependent Aftershock Risk Performance-Based Earthquake Engineering*, PEER Report 2005/13. Pacific Earthquake Engineering Research Center, Berkeley, CA.

Chapter 3 - SEQUENCE-BASED PROBABILISTIC SEISMIC HAZARD ANALYSIS

This chapter is derived from the following paper:

Iervolino I., Giorgio M., Polidoro B. (2014). Sequence-based probabilistic seismic hazard analysis. Bulletin of the Seismological Society of America. doi: 10.1785/0120130207 (in press).

3.1. Introduction

The probabilistic seismic hazard analysis (PSHA; e.g., McGuire, 2004) is a consolidated procedure to assess the seismic threat for a specific site. PSHA, in its classical format, refers to the occurrence of mainshocks. These are prominent magnitude earthquakes possibly identified within sequences of events concentrated both in space and time (i.e., clusters).

On the other hand, aftershocks in the sequence may be seen as triggered by the mainshock. The features of each sequence are considered to depend only on the magnitude and location of the triggering event, being conditionally independent (in stochastic sense) of the past history. On these premises, Yeo and Cornell (2009) developed aftershock-PSHA (APSHA) to express aftershock hazard similar to the mainshock hazard. Indeed, APSHA results are in terms of rate of exceedance of a ground motion intensity measure (IM) threshold. This is useful in the post-mainshock emergency phase; see Yeo and Cornell (2005) for a discussion.

It may be argued that the occurrence of clusters can be probabilistically described by the same stochastic process adopted to count the main events. In this context, it is assumed that the occurrence time for each cluster coincides with that of the triggering

earthquake. Indeed, starting from Toro and Silva (2001) and Boyd (2012), it appears possible to extend PSHA multiplying the rate of occurrence of mainshocks by the probability that a ground motion intensity measure threshold is exceeded at least once during the sequence. This means filtering the rate of occurrence of the clusters retaining only those causing the sought exceedance event.

From the engineering point of view, computing the rate of the event referring to the exceedance of a ground motion intensity level (e.g., that critical to a structure) during the sequence, factually means to also consider the chance that an aftershock causes structural failure, while the mainshock did not. This leads to sequence-based PSHA, or SPSHA, which may be relevant for performance-based seismic design. It allows to determine the exceedance rate of the design intensity accounting for the aftershock potential (Iervolino et al., 2013a). As per common practice of current seismic codes, damage accumulation on the structure is neglected, while it may be of interest for short-term risk management; see Yeo and Cornell (2005) and Iervolino et al. (2013b) for some result in this direction.

The study presented in the following, starting from the intuitions of the mentioned studies, derives the analytical formulation of SPSHA, that is including aftershocks in the hazard integral, which was still missing in Toro and Silva (2001) and Boyd (2012). It is built on the hypotheses that occurrence of mainshocks is regulated by a homogenous Poisson process (HPP), whereas occurrence of aftershocks is regulated by a conditional non-homogenous Poisson process (NHPP). It is assumed that: the rate of occurrence of the aftershocks pertaining to a given sequence, their magnitude range, and their spatial clustering, only depend on magnitude and location of the triggering mainshock. In the study foreshocks are neglected, as they are usually very limited in number (Yeo and Cornell, 2009).

Because, as illustrated in the following, the model for aftershocks is based on the modified Omori law (Utsu, 1961), the study may be seen as modeling primary aftershocks. In fact, other models as epidemic-type aftershock sequences (ETAS; e.g., Ogata, 1988) are virtually able to model clusters in which each event is able to generate its own sequence.

The study will not directly deal with issues related to the declustering of earthquakes, which will appear only in terms of the resulting occurrence rate of mainshocks and the parameters of the modified Omori law that are input data for the proposed model. On the other hand, it is to recall that results obtained for both mainshocks and aftershocks are model-dependent. This is because, given the original catalog, clustering is performed on the basis of conventional rules, which are defined via the model one adopts to describe the occurrence of earthquakes.
The chapter is structured such that PSHA and APSHA essentials are briefly reviewed first. Then, the combination of the two is analytically discussed to account for the effect of the whole sequence in a single hazard integral. The merely illustrative application, considering a generic seismogenic source, is finally carried out to compute the annual rate of exceedance of different IM-levels by means of SPSHA, and to evaluate the significance of differences with respect to classical seismic hazard analysis, in which the effects of aftershocks are neglected.

3.2. Mainshock, aftershocks, and ground motion intensity

In this section, stochastic processes and analytical formulations used to evaluate mainshock and conditional aftershock hazard, both expressed in terms of rate of exceedance of a ground motion intensity threshold, are briefly reviewed.

3.2.1. Mainshock probabilistic seismic hazard analysis

Probabilistic seismic hazard analysis usually adopts the homogeneous Poisson process to probabilistically model the number of earthquakes the seismic source produces. HPP is an independent- and stationary-increment (i.e., memory-less) process, entirely described by one parameter, the rate, ν_E. According to HPP, the number of events, N_E, occurring in the time interval of interest, $(t, t+\Delta T)$, is independent of the history of earthquakes occurred in the past and has the Poisson probability mass function in Equation (3.1).

$$P\left[N_E\left(t,t+\Delta T\right)=n\right]=P\left[N_E\left(\Delta T\right)=n\right]=\frac{\left(\nu_E\cdot\Delta T\right)^n}{n!}\cdot e^{-\nu_E\Delta T} \tag{3.1}$$

It is also consequent to the HPP that the interarrival time distribution of mainshocks is an exponential distribution, where the mean time between arrivals is the reciprocal of the rate.

In PSHA, at a site of interest, the exceedance of an IM threshold, im, is also probabilistically described by a HPP (Cornell, 1968). The rate of exceedance of im, $\lambda_{im,E}$, is obtained from ν_E via Equation (3.2), where the term $P\left[IM>im\,|\,x,y\right]$, provided by a ground motion prediction equation (GMPE), represents the probability that the intensity threshold is exceeded given an earthquake of magnitude $M_E=x$, from which the site is separated by a distance $R_E=y$.

$$\lambda_{im,E}=\nu_E\cdot\int_{r_{E,\min}}^{r_{E,\max}}\int_{m_{E,\min}}^{m_{E,\max}}P\left[IM>im\,|\,x,y\right]\cdot f_{M_E,R_E}\left(x,y\right)\cdot dx\cdot dy \tag{3.2}$$

The term f_{M_E,R_E} is the joint probability density function (PDF) of mainshock magnitude and distance random variables (RVs). In the case of a single source, if these two RVs may be considered stochastically independent, f_{M_E} is often described by a Gutenberg-Richter (GR) relationship (Gutenberg and Richter, 1944), and f_{R_E} is obtained on the basis of the source-site geometrical configuration. The integral limits are the magnitudes bounding the GR relationship and the distances defining the domain of possible R_E values (e.g., Reiter, 1990).

3.2.2. Aftershock probabilistic seismic hazard analysis

APSHA is also expressed in terms of rate of occurrence of events exceeding a ground motion intensity measure threshold at a site of interest. The main difference with respect to PSHA is that such a rate is time-variant. The expected number of events per unit time decreases as the time elapsed since the triggering mainshock increases. In this

sense, the process that describes occurrence of aftershocks is conditional to occurrence and characteristics of the mainshock.

The NHPP process adopted to build APSHA is based on the hypothesis that the daily rate of occurrence of the aftershocks, $\nu_{A|m_E}(t)$, can be expressed as in Equation (3.3), where t indicates the time elapsed since the occurrence of the triggering mainshock, which according to the adopted time scale, occurred at $t=0$. The model also assumes that magnitude of aftershocks is bounded between a minimum value of interest, $m_{\min}$, and that of the triggering mainshock. Coefficients *a* and *b* are from a suitable GR relationship, while *c* and *p* are from the modified Omori law (Utsu, 1961) for the considered sequence. Finally, given the intensity of the triggering mainshock, intensities of the aftershocks in the sequence are assumed to be stochastically independent random variables.

$$\nu_{A|m_E}(t)=\left(10^{a+b\cdot(m_E-m_{\min})}-10^{a}\right)\Big/\left(t+c\right)^{p} \tag{3.3}$$

From Equation (3.3) it follows that the expected number of aftershocks in the $(t,t+\Delta T_A)$ interval, is given by Equation (3.4).

$$\begin{aligned} &E\left[N_{A|m_E}(t,t+\Delta T_A)\right]= \\ &=\int_{t}^{t+\Delta T_A}\nu_{A|m_E}(\tau)\cdot d\tau=\frac{10^{a+b\cdot(m_E-m_{\min})}-10^{a}}{p-1}\cdot\left[\left(t+c\right)^{1-p}-\left(t+\Delta T_A+c\right)^{1-p}\right] \end{aligned} \tag{3.4}$$

Similar to PSHA, also APSHA filters the intensity of the process reducing the rate of occurrence of the events multiplying it by the (time-invariant) probability that the IM at the site of interest exceeds the threshold. This leads to the rate of the NHPP process, $\lambda_{im,A|m_E}(t)$, as in Equation (3.5), where f_{M_A,R_A} is the joint PDF of magnitude and source-to-site distance of the generic aftershock.

$$\lambda_{im,A|m_E}(t) = \nu_{A|m_E}(t) \cdot \int_{r_{A,\min}}^{r_{A,\max}} \int_{m_{\min}}^{m_E} P[IM > im \mid w,z] \cdot f_{M_A,R_A}(w,z) \cdot dw \cdot dz \tag{3.5}$$

Same considerations given in the previous section for f_{M_E,R_E} also apply to f_{M_A,R_A}. Aftershock location, and then source-to-site distance and its limiting values $\{r_{A,\min}, r_{A,\max}\}$, will be discussed later on. Indeed, despite the symbols in Equation (3.5), consistent with those of Yeo and Cornell (2009), the rate of exceedance of IM also depends on mainshock location.

3.3. Combining mainshocks and conditional aftershocks stochastic processes

In this section the probabilistic seismic hazard analysis accounting for the effects of both mainshock and aftershocks is formulated. The occurrence of sequences is described by a HPP process and, within a sequence, occurrence of aftershocks is described by a NHPP, the rate function of which is conditional to the magnitude of the triggering event. The aim is, again, to evaluate the annual rate, λ_{im}, of exceedance of a ground motion intensity measure.

Herein, such a rate accounts for the occurrence of events defined as the exceedance of an *IM* threshold at least once within a sequence, Equation (3.6).

$$\begin{aligned} &\lambda_{im} = \nu_E \cdot P[IM > im] = \nu_E \cdot P[IM_E > im \cup IM_{\cup A} > im] = \\ &= \nu_E \cdot \{1 - P[IM_E \le im \cap IM_{\cup A} \le im]\} \end{aligned} \tag{3.6}$$

In the equation, *IM* is the maximum ground motion intensity among all events in the cluster, IM_E is the mainshock intensity measure, and $IM_{\cup A}$ indicates the maximum intensity among the aftershocks. Indeed, $IM_{\cup A}$ exceeds the threshold if and only if at least one aftershock produces intensity above the threshold at the site.

According to APSHA, the features of the aftershock sequence entirely depend on the characteristics of the mainshock. The number of events, their magnitude, and their location, are function of the size and location of the sequence-triggering earthquake. Therefore, conditional to magnitude and location of the mainshock, the two events defined as the *IM* threshold is not exceeded: (1) in the mainshock, and (2) in any of the aftershocks, are stochastically independent, Equation (3.7). (Note that this, which follows from the PSHA and APSHA models, is also consistent with Boyd, 2012).

$$\begin{aligned}\lambda_{im} &= \nu_E \cdot \left\{ 1 - \iint_{M_E, R_E} P\left[IM_E \le im \cap IM_{\cup A} \le im \mid x, y \right] \cdot f_{M_E, R_E}(x, y) \cdot dx \cdot dy \right\} = \\ &= \nu_E \cdot \left\{ 1 - \iint_{M_E, R_E} P\left[IM_E \le im \mid x, y \right] \cdot P\left[IM_{\cup A} \le im \mid x, y \right] \cdot f_{M_E, R_E}(x, y) \cdot dx \cdot dy \right\}\end{aligned} \tag{3.7}$$

The probability of not exceeding the threshold during the aftershock sequence is formulated accounting for the fact that such a sequence is comprised of a random number of events, N_A. According to the NHPP assumption, such a random variable is Poisson distributed, as in Equation (3.1), yet with mean given in Equation (3.4). Therefore, applying the total probability theorem to the $P\left[IM_{\cup A} \le im \mid x, y \right]$ term in Equation (3.7), Equation (3.8) results.

$$\lambda_{im} = \nu_E \cdot \left\{ 1 - \iint\limits_{M_E,R_E} P\left[IM_E \le im \mid x,y\right] \cdot \right.$$
$$\left. \cdot \sum_{i=0}^{+\infty} P\left[IM_{\cup A} \le im \mid x,y,i\right] \cdot P\left[N_A = i \mid x\right] \cdot f_{M_E,R_E}(x,y) \cdot dx \cdot dy \right\} =$$
$$= \nu_E \cdot \left\{ 1 - \iint\limits_{M_E,R_E} P\left[IM_E \le im \mid x,y\right] \cdot \right.$$
$$\left. \cdot \sum_{i=0}^{+\infty} \left(P\left[IM_A \le im \mid x,y\right] \right)^i \cdot P\left[N_A = i \mid x\right] \cdot f_{M_E,R_E}(x,y) \cdot dx \cdot dy \right\} =$$
$$= \nu_E \cdot \left\{ 1 - \iint\limits_{M_E,R_E} P\left[IM_E \le im \mid x,y\right] \cdot \right.$$
$$\left. \cdot \sum_{i=0}^{+\infty} \left(P\left[IM_A \le im \mid x,y\right] \right)^i \cdot \frac{\left(\int_0^{\Delta T_A} \nu_{A|x}(\tau) \cdot d\tau \right)^i}{i!} \cdot e^{-\int_0^{\Delta T_A} \nu_{A|x}(\tau) \cdot d\tau} \cdot f_{M_E,R_E}(x,y) \cdot dx \cdot dy \right\} \quad (3.8)$$

In the equation, $P\left[IM_{\cup A} \le im \mid x,y,i\right] = 1$ for $i = 0$. $\nu_{A|x}$ reflects the fact that such a rate depends on the mainshock magnitude, and ΔT_A is the duration of the aftershock sequence (the value assumed for this parameter may affect the result of SPSHA as the larger ΔT_A, the larger the mean of the N_A RV, thus the larger the resulting *IM* exceedance rate). $P\left[IM_A \le im \mid x,y\right]$, equal for all aftershocks as per APSHA (Yeo and Cornell, 2009), is the non-exceedance probability of the intensity threshold in the generic aftershock, marginal with respect to its possible magnitude and location, yet given magnitude and location of the mainshock.

Given magnitude and location of the aftershock, the probability the *IM* threshold is not exceeded is conditionally independent of the mainshock. Then, reformulating the $P\left[IM_A \le im \mid x,y\right]$ term in Equation (3.8) via the total probability theorem, Equation (3.9) results.

$$\lambda_{im} = \nu_E \cdot \left\{ 1 - \iint\limits_{M_E, R_E} P\left[IM_E \le im \mid x, y\right] \cdot \right.$$
$$\cdot \sum_{i=0}^{+\infty} \left(\iint\limits_{M_A, R_A} P\left[IM_A \le im \mid w, z\right] \cdot f_{M_A, R_A \mid M_E, R_E}\left(w, z \mid x, y\right) \cdot dw \cdot dz \right)^i \cdot \tag{3.9}$$
$$\left. \cdot \frac{\left(E\left[N_{A|x}\left(0, \Delta T_A\right)\right]\right)^i}{i!} \cdot e^{-E\left[N_{A|x}\left(0, \Delta T_A\right)\right]} \cdot f_{M_E, R_E}\left(x, y\right) \cdot dx \cdot dy \right\}$$

In the equation, the $P\left[IM_A \le im \mid w, z\right]$ term is the non-exceedance probability of *im* in the generic aftershock of known magnitude and location, and $f_{M_A, R_A \mid M_E, R_E}$ is the magnitude and distance joint PDF of an aftershock, conditional to the features of the mainshock. This PDF accounts for the dependence, of both magnitude of the aftershocks and size/location of the seismogenic zone for aftershocks, on magnitude and location of the triggering mainshock (to follow). The integration limits are those of Equation (3.2) and Equation (3.5) for mainshock and aftershocks, respectively.
A more compact expression of the hazard integral is given by Equation (3.10).

$$\lambda_{im} =$$
$$= \nu_E \cdot \left\{ 1 - \iint\limits_{M_E, R_E} P\left[IM_E \le im \mid x, y\right] \cdot P\left[IM_{\cup A} \le im \mid x, y\right] \cdot f_{M_E, R_E}\left(x, y\right) \cdot dx \cdot dy \right\} =$$
$$= \nu_E \cdot \left\{ 1 - \iint\limits_{M_E, R_E} P\left[IM_E \le im \mid x, y\right] \cdot e^{-P\left[IM_A > im \mid x, y\right] \cdot \int_0^{\Delta T_A} \nu_{A|x}(\tau) \cdot d\tau} \cdot f_{M_E, R_E}\left(x, y\right) \cdot dx \cdot dy \right\} = \tag{3.10}$$
$$= \nu_E \cdot \left\{ 1 - \iint\limits_{M_E, R_E} P\left[IM_E \le im \mid x, y\right] \cdot \right.$$
$$\left. e^{-E\left[N_{A|x}\left(0, \Delta T_A\right)\right] \cdot \iint_{M_A, R_A} P\left[IM_A > im \mid w, z\right] \cdot f_{M_A, R_A \mid M_E, R_E}\left(w, z \mid x, y\right) \cdot dw \cdot dz} \cdot f_{M_E, R_E}\left(x, y\right) \cdot dx \cdot dy \right\}$$

In fact, Equation (3.10) is obtained using the equality in Equation (3.11).

$$\sum_{i=0}^{+\infty}\left(\iint_{M_A,R_A} P\left[IM_A \le im \mid w,z\right]\cdot f_{M_A,R_A|M_E,R_E}\left(w,z \mid x,y\right)\cdot dw\cdot dz\right)^i \cdot \frac{\left(E\left[N_{A|x}\left(0,\Delta T_A\right)\right]\right)^i}{i!}\cdot$$
$$\cdot e^{-E\left[N_{A|x}\left(0,\Delta T_A\right)\right]} =$$
$$= e^{-E\left[N_{A|x}\left(0,\Delta T_A\right)\right]\cdot\left(1-\iint_{M_A,R_A} P\left[IM_A\le im|w,z\right]\cdot f_{M_A,R_A|M_E,R_E}\left(w,z|x,y\right)\cdot dw\cdot dz\right)} = \tag{3.11}$$
$$= e^{-E\left[N_{A|x}\left(0,\Delta T_A\right)\right]\cdot\left(\iint_{M_A,R_A} P\left[IM_A> im|w,z\right]\cdot f_{M_A,R_A|M_E,R_E}\left(w,z|x,y\right)\cdot dw\cdot dz\right)}$$

It is to note that the result in Equation (3.10) could also be directly obtained, computing the probability of zero aftershocks causing the exceedance in $\left(0,\Delta T_A\right)$, via a NHPP of rate in Equation (3.5). Nevertheless, derivation given allows deeper insights into the implications of the assumptions on the aftershock process on the hazard integral.

Having formulated the hazard integral for the cluster in the case of a single source, it may be worth to briefly discuss the common case of multiple (independent) sources contributing to the hazard of the site of interest. In the case for each of these the occurrence of mainshocks is modeled via a HPP, the resulting rate is just the summation, over all the sources, of the rates from Equation (3.9). If the occurrence of mainshocks is probabilistically described by means of other processes, for example a renewal process, then the rate of exceedance may not be time-invariant (see Polidoro et al., 2013, for a discussion). In such cases, if the modified Omori law still applies for aftershocks, then it is possible to write the equations for the exceedance probability within the cluster similar to this study, yet the resulting formulation will be certainly different.

It is also to note that the proposed approach could be also extended to the case in which alternate models, such as the ETAS (e.g., Ogata, 1988), accounting for the possibility of any earthquake in the cluster to generate its own sequence, are employed in lieu of the modified Omori law to describe the seismic sequences. These models lead to change the rate of occurrence of aftershocks and possibly affect also that of mainshocks.

3.4. Illustrative application

As an illustrative application of SPSHA, hazard was computed for a site in the middle of a generic seismic source represented by an area, the size of which is $30 \times 100\, km^2$ (Figure 3.1).

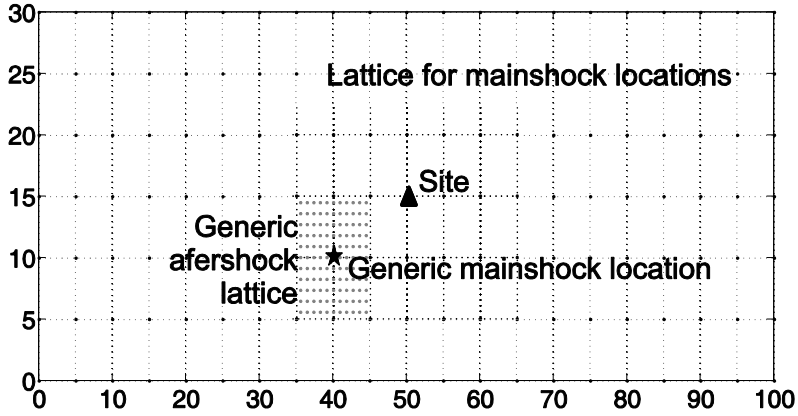

Figure 3.1. Seismogenic source lattice for mainshocks, generic aftershock lattice around the epicenter of a mainshock, and site of interest.

3.4.1. Characteristics of the mainshock and of the conditional aftershock sequence

Mainshock epicenters were assumed as uniformly distributed in the areal seismic source of Figure 3.1, which was discretized by $5 \times 5\, km^2$ lattice for computational purposes. Mainshock rate was, arbitrarily, assumed to be $\nu_E = 0.054\ \ events / yr$.

The magnitude distribution of mainshock was, arbitrarily again, chosen to be a truncated exponential defined in the $[4.3, 5.8]$ range, as illustrated in Figure 3.2. The *b*-value of the GR relationship for mainshocks is 1.056.

In the application, magnitude and source-to-site distance were considered to be independent RVs.

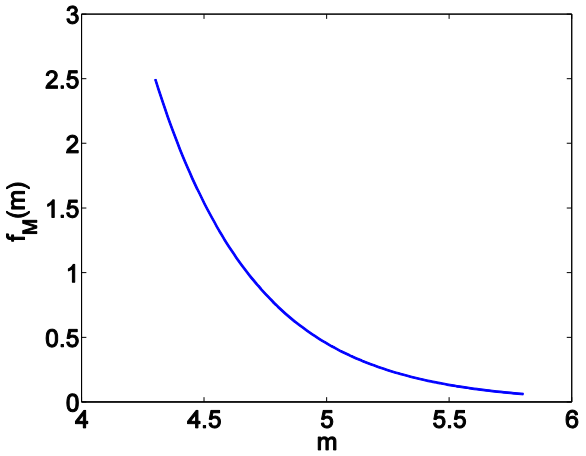

Figure 3.2. Magnitude distribution for mainshocks

It was assumed that each mainshock has aftershocks constrained in an area around its epicenter. The size of the seismogenic zone for aftershocks in squared kilometers, S_A, depends on the magnitude of the main event via Equation (3.12) (Utsu, 1970); Figure 3.3.

$$S_A = 10^{(m_E - 4.1)} \tag{3.12}$$

Within this area, arbitrarily assumed to be a square and discretized by means of a 121 points lattice, epicenters are uniformly distributed (see Figure 3.1). In fact, the proposed approach to hazard may deal with any shape of the aftershock source area (e.g., with an ellipsoidal shape, which is often considered) and/or any function representing the probability of each grid cell of such area being the location of an aftershock (e.g., probability density functions that have a bell-shaped radial decay from the mainshock location, such as in Zhuang et al., 2002). However, this issue does not significantly affect the conclusions of the study, and therefore the uniform distribution in the square was considered for simplicity.

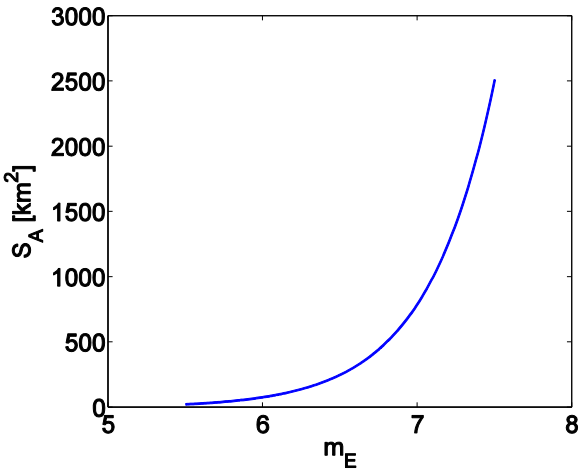

Figure 3.3. Mainshock magnitude versus aftershock source area.

The parameters used in the modified Omori law and in the Gutenberg-Richter relationship for aftershocks, that is the parameters of Equation (3.3), were taken from Lolli and Gasperini (2003): $a = -1.66$, $b = 0.96$, $c = 0.03$ (in days), $p = 0.93$, and $m_{\min} = 4.2$.

These apply to Italian generic aftershock sequences; Yeo and Cornell (2009), for example, use another set of parameters representing the equivalent California model.

To evaluate both the $P\left[IM_E \le im \,|\, m, r\right]$ and the $P\left[IM_A \le im \,|\, m, r\right]$ terms, the Ambraseys et al. (1996) GMPE was used; therefore, the magnitude scale to be considered is that of this GMPE. Ambraseys et al. (1996) use the R_{jb} distance metric, which is the distance to the surface projection of the source (Joyner and Boore, 1981). On the other hand, because the points in Figure 3.1 are considered to be epicenters of mainshocks, the relationship in Gruppo di Lavoro (2004), Equation (3.13), was used to retrieve the value of R_{jb} (in *km*) to be plugged in the GMPE, converting from the epicentral distance, *R*, which is identified by R_E or R_A in the hazard integrals above.

$$R_{jb} = -3.5525 + 0.8845 \cdot R \tag{3.13}$$

3.4.2. Cases and Results

Given the working assumptions taken for the application, SPSHA was computed according to Equation (3.10). In performing this first exercise, the *IM* was considered to be the PGA (peak ground acceleration) on rock. Moreover, following Yeo and Cornell (2009), the duration of the aftershock sequence (ΔT_A) was considered arbitrarily (Yeo, personal communication, 2013) equal to 90 days since the mainshock occurrence.

Figure 3.4 compares the SPSHA results, in terms of annual rate of exceedance of different PGA thresholds, to those obtained via PSHA using Equation (3.2), that is accounting only for mainshocks. Indeed, in Figure 3.5 the relative difference between the SPSHA and PSHA, in terms of rate, is also depicted. Even if hazard curves appear close differences up to 30% in rates may be observed.

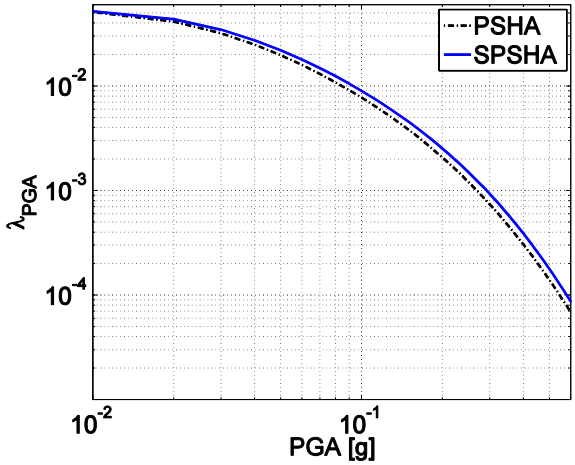

Figure 3.4. PSHA and SPSHA results in terms of PGA for the illustrative application.

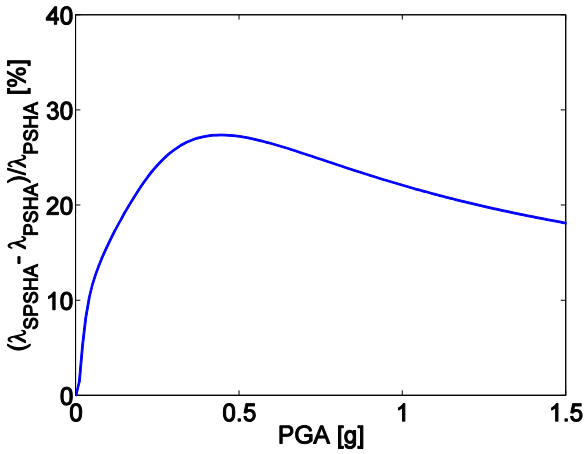

Figure 3.5. PSHA and SPSHA differences in terms of PGA for the illustrative application.

Because the 5% damped pseudo-spectral-acceleration, $Sa(T)$, is an *IM* of general earthquake engineering interest, SPSHA was also computed in terms of this intensity measure, with T (structural period) varying in the 0s-2s range. Results of this further analysis are expressed in terms of uniform hazard spectrum (UHS) that is a spectrum the ordinates of which all have the same exceedance probability in a given time frame, or equivalently the same return period (e.g., Reiter, 1990). In Figure 3.6, the UHS referring to 475 yr, a typical life-safety-related design return period for ordinary structures, is compared with its PSHA counterpart. Figure 3.7 shows the relative differences between the spectra computed via SPSHA and PSHA. Note that in this case comparison is in terms of *IM* given the return period (rather than rate as in the previous example) and changes up to 10% are observed.

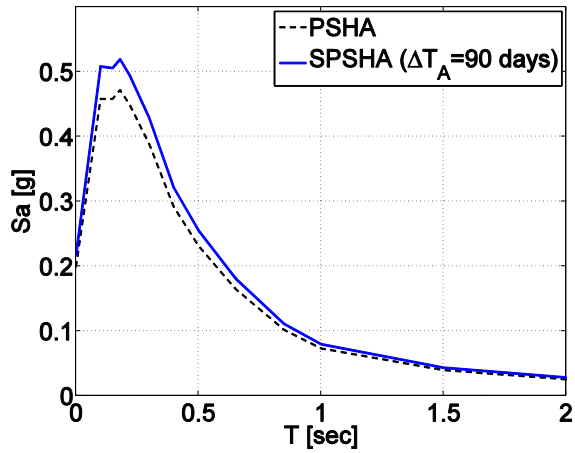

Figure 3.6. PSHA and SPSHA illustrative application results in terms of 475 yr UHS, that is 5% damped pseudo-spectral acceleration versus oscillation period, where all ordinates share the same 10% in 50 yr exceedance probability.

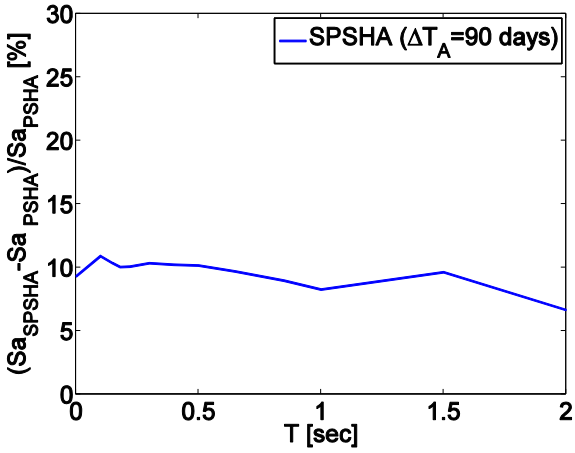

Figure 3.7. PSHA and SPSHA differences in terms of 475 yr UHS for the illustrative application.

These results, in terms of changes in both rates and accelerations, are comparable to those found by Boyd (2012), even though the differences in the two studies and applications (Boyd, personal communication, 2013).

3.4.3. Further comparative examples

Further examples have been carried out to highlith the influence of some parameters and functions used in the previous section. In particular, the duration of the aftershock sequence and the distribution of the aftershocks location have been considered.

About the first aspect, SPSHA analysis both in terms of annual rate of exceedance of PGA and UHS have been conducted considering different ΔT_A values. Figure 3.8 shows hazard in terms of annual rate of exceedance of different thresholds when PGA (peak ground acceleration on rock) is the *IM*. The figure refers to the hazard considered only in terms of mainshocks, that is Equation (3.2), and considering also aftershocks according to Equation (3.10). The aftershocks durations (ΔT_A) considered are: 15 days, 90 days, 1 year and 3 years since the time of occurrence of the mainshock.

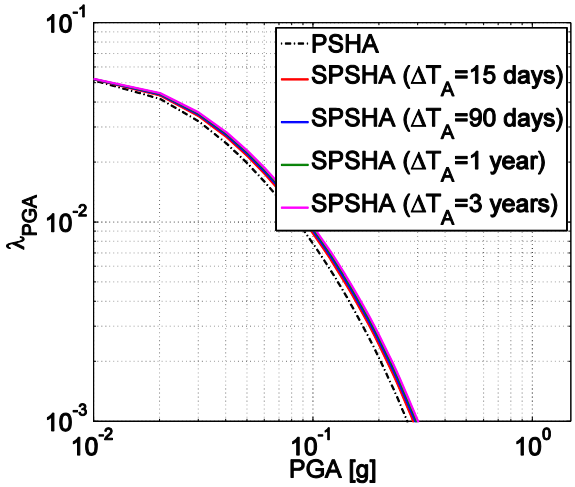

Figure 3.8. PSHA and SPSHA results in terms of PGA for the illustrative application.

In Figure 3.9 the relative difference between the SPSHA (evaluated for the different ΔT_A values) and PSHA in terms of annual rate of exceedance is also depicted. It can be noted that differences have the same trend and they increase with the increasing aftershocks duration (ΔT_A). In fact, with the increasing of ΔT_A also the expected

number of aftershocks increases, hence, the probability that the intensity measure is exceeded.

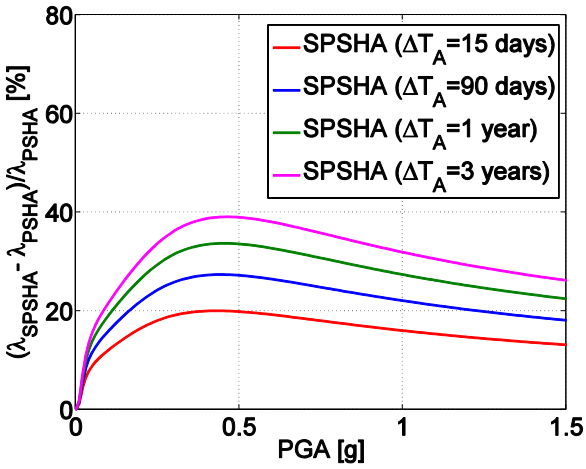

Figure 3.9. PSHA and SPSHA differences in terms of PGA for the illustrative application.

As a further analysis, SPSHA was also computed taking the 5% damped pseudo-spectral-acceleration, $Sa(T)$, in the 0s-2s range of periods, as an IM. In Figure 3.10 the resulting 475 yr return period uniform hazard spectra obtained for the different aftershocks durations are compared with the PSHA counterpart.

Figure 3.11 shows the relative difference between the SPSHA and PSHA acceleration spectra. It can be noted that for a fixed (ΔT_A) value differences are almost constant, while they increase with the increasing aftershocks duration.

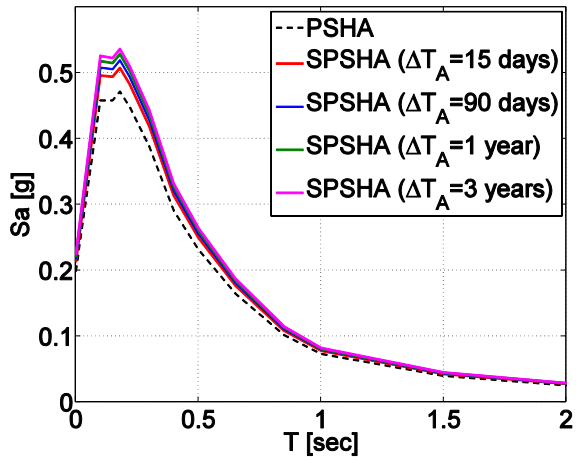

Figure 3.10. PSHA and SPSHA results in terms of 475 yr UHS varying the duration of the sequence for the illustrative application.

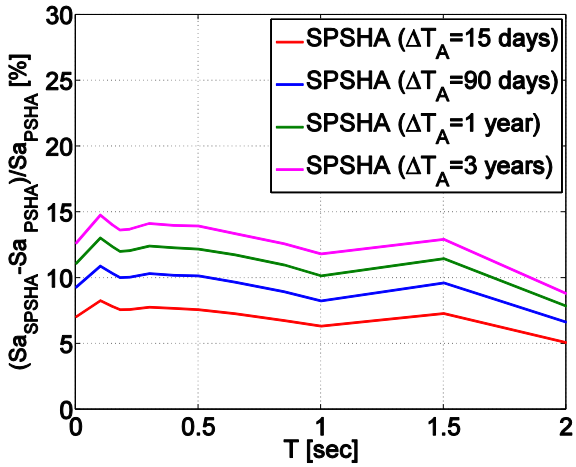

Figure 3.11. PSHA and SPSHA differences in terms of 475 yr UHS varying the duration of the sequence for the illustrative application.

In the previous section, it was assumed that each mainshock has aftershocks constrained in an area around its epicenter. The size of the seismogenic zone for aftershocks depends on the magnitude of the main event via Equation (3.12) and within

this area, epicenters are uniformly distribute (U_{pdf}). In this section another possible distribution (a bivariate Gaussian distribution, BG_{pdf}) is considered, Equation (3.14), where *x* and *y* indicate the aftershock location, while d and α are the parameters of the distribution assumed arbitrarly equal to $d = 0.121 \cdot 10^{-2}$ degrees^2 and $\alpha = 0.972$ magnitude^{-1}.

$$f(x,y \mid m) = \frac{1}{2 \cdot \pi \cdot d \cdot e^{\alpha \cdot (m - m_{\min})}} \cdot e^{-\frac{x^2 + y^2}{2 \cdot d \cdot e^{\alpha \cdot (m - m_{\min})}}} \tag{3.14}$$

Figure 3.12 compares the SPSHA results (considering both a uniform and a bivariate gaussian distributions), in terms of annual rate of exceedance of different PGA thresholds, to those obtained via PSHA using Equation (3.2), that is accounting only for mainshocks; in both cases aftershocks duration is assumed equal to $\Delta T_A = 90$ days.

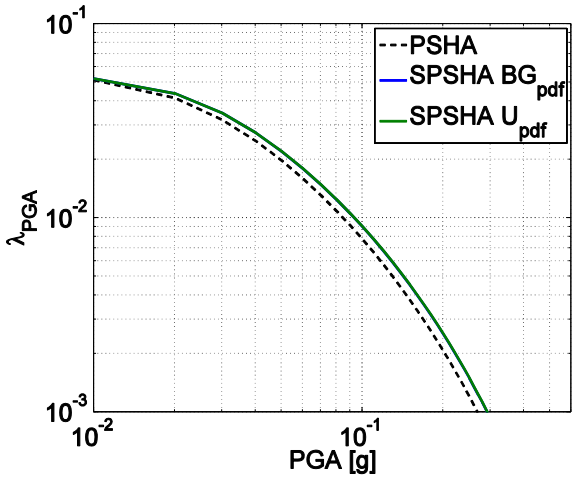

Figure 3.12. PSHA and SPSHA(considering for aftershock location both a uniform and a bivariate Gaussian distribution) results in terms of PGA for the illustrative application.

In Figure 3.13 the relative difference between the SPSHA and PSHA, in terms of rate, is also depicted. Results show that a different distribution for the aftershocks location leads to similar results in terms of annual rate of exceedance of different PGA values.

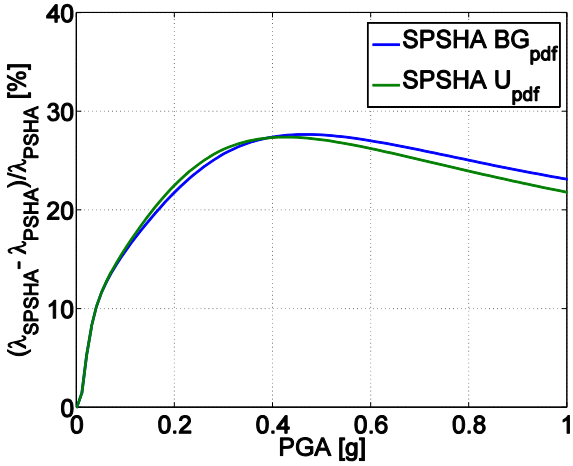

Figure 3.13. PSHA and SPSHA differences in terms of PGA for the illustrative application.

Results of this further analysis are also expressed in terms of uniform hazard spectrum referring to a return period equal to 475 yr., Figure 3.14.

Figure 3.15 shows the relative differences between the spectra computed via SPSHA considering both a uniform and bivariate Gaussian distribution and PSHA. Results, show that differences between the two cases are negligible.

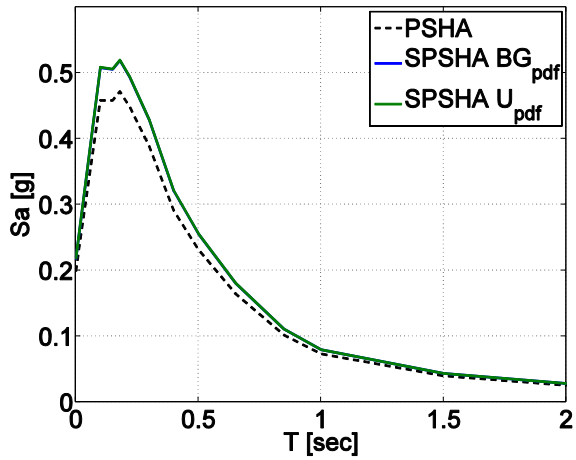

Figure 3.14. PSHA and SPSHA (considering for aftershock location both a uniform and a bivariate Gaussian distribution) results in terms of 475 yr UHS for the illustrative application.

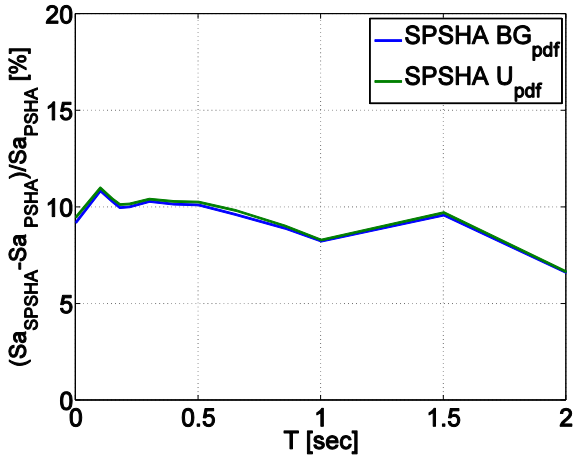

Figure 3.15. PSHA and SPSHA differences in terms of 475 yr UHS for the illustrative application.

3.5. Conclusions

The study presented in this chapter aimed at contributing to the inclusion of Omori-type aftershocks, to main earthquake events, in the seismic hazard analysis expressed in terms of rate of exceedance of a ground motion intensity measure. The focus was the probabilistically consistent formalization of the hazard integral, looking at the event of exceeding an intensity threshold at least once during the sequence.

To directly extend seismic hazard including the aftershock potential in the computation of the exceedance rate may be useful for performance-based design, as the intensity critical to the structure of interest could be exceeded in any of the earthquakes of the cluster.

Probabilistic seismic hazard analysis for mainshock-aftershocks seismic sequences was built on the homogeneous Poisson process assumption for occurrence of mainshocks, and on the conditional non-homogeneous Poisson process for the occurrence of aftershocks. The latter depends on the features of the mainshock via the modified Omori law and via a semi-empirical relationship between the mainshock characteristics and the aftershock source area.

Sequence-based PSHA was formulated analytically considering that the effects of aftershocks (i.e., ground motion intensities) are conditionally independent on everything happens outside the cluster, given the magnitude and location of the triggering mainshock.

The illustrative application refers to a generic source zone for mainshocks and to a generic aftershock sequence. The SPSHA was compared to the classical PSHA results, both in terms of rates given the *IM* threshold, and in terms of *IM* given the return period. Results, at least for the case set up, indicate changes up to about 30% in PGA rate and up to about 10% in pseudo-spectral acceleration values corresponding to the 475 yr return period.

Further examples have been carried out to highlith the influence of some parameters. In particular, a variation in terms of aftershock sequence duration and distribution of the aftershocks location have been investigated. Dealing with the first aspect, SPSHA analysis both in terms of annual rate of exceedance of PGA and UHS have been

conducted considering different aftershocks durations. Results indicate that, as with the increasing aftershock duration, the expected number of aftershocks improves, also the hazard expressed both in terms of annual rate of exceedance of PGA values and UHS rises.

Finally, SPSHA results obtained considering a uniform distribution for the aftershocks location is compared with the case a bivariate Gaussian distribution is adopted. Analysis shows that the distributions lead to similar results.

It is believed that the derived formulation may be of earthquake engineering interest, especially with respect to long-term performance-based design and assessment of structures.

References

Ambraseys NN, Simpson KA and Bommer JJ (1996). Prediction of horizontal response spectra in Europe, *Earthq. Eng. Struct. D.* **25**, 371-400.

Boyd OS (2012). Including Foreshocks and Aftershocks in Time-Independent Probabilistic Seismic-Hazard Analyses, *B. Seismol. Soc. Am.* **102**, 909-917.

Cornell CA (1968). Engineering Seismic Risk Analysis, *B. Seismol. Soc. Am.* **58**, 1583-1606.

Gruppo di Lavoro (2004). *Redazione della Mappa di Pericolosità Simica Prevista dall'Ordinanza PCM 3274 del 20 Marzo 2003, Rapporto conclusivo per il Dipartimento della Protezione Civile*. Istituto Nazionale di Geofisica e Vulcanologia, Rome, Italy. (in Italian)

Gutenberg B and Richter CF (1944). Frequency of earthquakes in California, *B. Seismol. Soc. Am.* **34**, 185-188.

Iervolino I, Giorgio M and Polidoro B (2013a). Probabilistic seismic hazard analysis for seismic sequences. Proc. of *Vienna Congress on Recent Advances in Earthquake Engineering and Structural Dynamics*, VEESD, Vienna, Austria, August 28-30.

Iervolino I, Giorgio M and Chioccarelli E (2013b). Closed-form aftershock reliability of damage-cumulating elastic-perfectly-plastic systems, *Earthq. Eng. Struct. D.* DOI: 10.1002/eqe.2363 (in press)

Joyner WB and Boore DM (1981). Peak horizontal acceleration and velocity from strong motion records including records from the 1979 Imperial Valley, California, earthquake, *B. Seismol. Soc. Am.* **71**, 2011-38.

Lolli B and Gasperini P (2003). Aftershocks hazard in Italy Part I: Estimation of time-magnitude distribution model parameters and computation of probabilities of occurrence, *J. Seismol.* **7**, 235–257.

McGuire RK (2004). *Seismic Hazard and Risk Analysis*, Earthquake Engineering Research Institute, MNO-10, Oakland, California.

Ogata Y (1988). Statistical models for earthquake occurrences and residual analysis for point processes, J. Am. Stat. Assoc. 83, 9–27.

Polidoro B, Iervolino I, Giorgio M, Chioccarelli E (2013). Models and issues in history-dependent mainshock hazard, Proc. of *11th Conference on Structural Safety and Reliability*, ICOSSAR '13, New York, US, June 16-20.

Reiter L (1990). *Earthquake hazard analysis: issues and insights*, Columbia University Press, New York.

Toro GR and Silva WJ (2001). Scenario earthquakes for Saint Louis, MO, and Memphis, TN, and seismic hazard maps for the central United States region including the effect of site conditions: Technical report to U.S. Geological Survey, Reston, Virginia, under Contract 1434-HQ-97-GR-02981.

Utsu T (1970). Aftershocks and earthquake statistics (1): Some parameters which characterize an aftershock sequence and their interrelations. Journal of the Faculty of Science, Hokkaido University, Series 7, Geophysics 3, 129-195.

Utsu T (1961). A statistical study on the occurrence of aftershocks, Geophys. Mag. 30, 521–605.

Yeo GL and Cornell CA (2005). *Stochastic characterization and decision bases under time-dependent aftershock risk in performance-based earthquake engineering*, PEER Report 2005/13, Pacific Earthquake Engineering Research Center, Berkeley, CA.

Yeo GL and Cornell CA (2009). A probabilistic framework for quantification of aftershock ground-motion hazard in California: Methodology and parametric study, *Earthq. Eng. Struct. D.* **38**, 45-60.

Zhuang J, Ogata Y and Vere-Jones D (2002). Stochastic Declustering of Space-Time Earthquake Occurrences, *J. Am. Stat. Ass.* **97**, 369-380.

Chapter 4 - RELIABILITY OF STRUCTURES TO EARTHQUAKE CLUSTERS

This chapter is derived from the following papers:

Iervolino I., Giorgio M., Polidoro B. (2014). Reliability of structures to earthquake clusters. (Under review).

Iervolino I., Giorgio M., Polidoro B. (2014). Accounting for the aftershock effect in the life-cycle assessment of structures. Second European Conference on Earthquake Engineering and Seismology (2ECEES), Istanbul, Turkey.

4.1. Introduction

Life-cycle models for structures require to account for time-variant issues possibly affecting the assessment of the risk of failure. In particular, the degradation over time of structural performance may need to be considered, and it is the focus of the study presented herein. Usually, literature distinguishes between two categories of phenomena which may lead to damage accumulation: (1) continuous deterioration of material characteristics (or aging) and (2) cumulating damage because of repeated overloading due to earthquake shocks (e.g., Sanchez-Silva et al., 2011). In a probabilistic framework, the only possible when dealing with the uncertainties affecting the life-cycle assessment of structures, these two issues require different stochastic modeling as: the former is likely to be represented by a process, which considers damages that cumulate continuously over time, while the latter can be more properly interpreted as the accumulation of the effect of repeated shocks that are point-in-time events with respect to the life-cycle of the structure.

The current best practice with respect to long-term seismic risk analysis of structures is certainly represented by the performance-based earthquake engineering framework (or PBEE; e.g., Cornell and Krawinkler, 2000). PBEE conveniently splits the structural assessment in sub-problems that can be more easily addressed, yet providing the sought result if combined: hazard, vulnerability, and loss (or exposure, that is the value of the elements at risk).

Classical probabilistic seismic hazard analysis (PSHA) usually refers to the homogeneous Poisson process (HPP) in order to model the temporal distribution of seismic shocks at the earthquake source and at the site of the construction of interest (e.g., McGuire, 2004). A memory-less model is also adopted to account for the spatial distribution of the earthquakes. One of the main limitation of this approach is that it is used to account for the occurrence of mainshocks only. Indeed, in a context where structural damage accumulation is tackled, it is to consider that aftershocks may have a non-negligible effect on the assessment of seismic risk and then on the life-cycle (Yeo and Cornell, 2009b). Unfortunately, this classical PSHA cannot be directly extended to model occurrence of all the seismic events. Indeed, both the use of the HPP (a process with independent and stationary increments) and the model adopted to describe spatial distribution of mainshocks, are not suited to model the occurrence of events that are clustered in time and space. In fact, these clusters include a mainshock (i.e., the largest magnitude event) and the following aftershock sequence, whose spatial and temporal distribution depends on the characteristics of the triggering mainshock.

Stochastic modeling of structures cumulating damage due to mainshock-aftershock seismic sequences is the issue addressed in the presented study. The work builds on recent results of the authors about stochastic modeling of degradation in earthquake resistant structures for life-cycle assessment (e.g., Iervolino et al., 2013a), short-term structural risk assessment based on aftershock probabilistic seismic hazard analysis (or APSHA; Yeo and Cornell 2009a), and damage accumulation in aftershock sequences (e.g., Iervolino et al. 2013b). In the study, earthquake clusters are considered instantaneous with respect to structural life; therefore, seismic events are described by a marked (or reward; Ross, 1996) point process, where each event is represented by its occurrence time (i.e., the occurrence time of the triggering mainshock) and damage

that it produces. The occurrence of earthquake clusters is modeled via the same HPP considered for the mainshocks (Boyd, 2012), while the random occurrence of aftershock is represented by means of a (conditional) non-homogeneous Poisson process (NHPP), the intensity of which depends on the characteristics of the sequence-triggering mainshock (Yeo and Cornell, 2009a). On the structural vulnerability side, it is considered that the structure may suffer damage both in the mainshock and in the following aftershocks, and that performance degradation due to these seismic damages can eventually lead to failure.

The main assumption of the model is that increments of damage accumulated over different seismic sequences are independent and identically distributed (i.i.d.) random variables (RVs), which are also independent of the process regulating occurrence of clusters. It is clear that the core reason for these assumptions is analytical convenience (to follow). Nonetheless, in the case of the considered application, they are less restrictive than it may appear; indeed, as it has been shown in Iervolino et al. (2013a-b) they are applicable to simple (yet of general application in the earthquake engineering context) elastic-perfectly-plastic (EPP) single degree of freedom (SDOF) systems, at least if energy-based damage indices are adopted. The model also explicitly accounts for the fact that not all earthquakes are damaging; i.e., it explicitly considers that some mainshocks and most of the aftershocks are not strong enough to induce energy dissipation in the structure.

The chapter is structured such that the compound Poisson process modeling structural damage accumulation is described first. Then, the damage variable selected to define the state of the stochastic model is briefly discussed. Subsequently, starting from the hypotheses taken for hazard and vulnerability, the distribution of damage in a single cluster (i.e., a single mainshock-aftershock sequence) is derived. Finally, the problem of formulating the reliability of the considered structure is addressed. Different solutions are obtained, each of which accounting for a specific state of knowledge about the seismic history of the structure. In developing these conditional reliabilities two different models are adopted to represent the damage in a single cluster: (a) the gamma and (b) the inverse-Gaussian. Main motivation for this is that the reproductive property of these RVs enables closed-form solutions, or at least closed-form

approximations, for all the considered scenarios. An illustrative application of the proposed methodology, to an EPP-SDOF structure located in an ideal seismic source zone, closes the chapter. For this simple structure the model is calibrated and the probability of failure is obtained. Results of the life-cycle assessment are also compared with those in the case aftershock effect is ignored.

4.2. Damage process formulation

The issue tackled in this study is sketched in Figure 4.1, where the vertical axis reports the residual seismic capacity as a function of time. The source of deterioration, in absence of aging, is related to damaging events in seismic sequences comprised of a mainshock and following aftershocks (foreshocks are neglected as they are usually very small in number, Yeo and Cornell 2009a). Aging is neglected herein for simplicity; the interested reader may refer to Iervolino et al. (2013a) for the combination of cumulative seismic damage and continuous deterioration consistent with the framework of this study. Considering that a seismic sequence, with duration in the order of months, may be seen as a point-in-time event with respect to the life-cycle of the structure, cluster occurrence time is considered coinciding with that of the triggering mainshock.

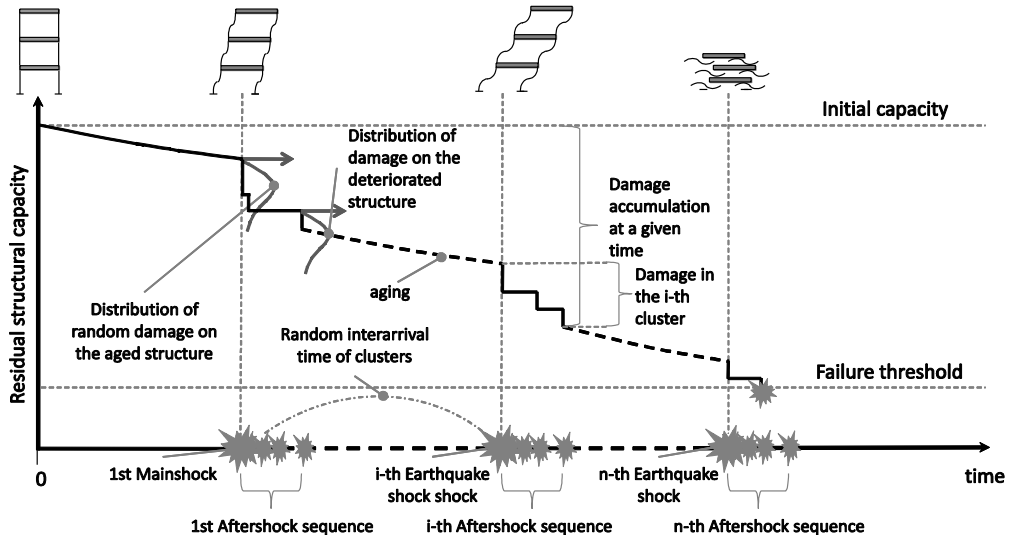

Figure 4.1. Sketch of degradation in structures subjected to seismic damages in mainshock-aftershocks sequences.

On the other hand, the effect of the (whole) sequence on the structure is evaluated considering the effective occurrence time and location of the triggering mainshock and all the aftershocks in the cluster. The advantage of this modeling approach stands in the fact that it allows describing the sequence effect as that of a single event, as schematically illustrated in Figure 4.2. Clearly, this approach works satisfactorily in the case repair is assumed unfeasible within a sequence.

Given a metric of the damage effect on the residual structural performance, for example the residual ductility to collapse, $\mu(t)$, the degradation process may be expressed as in Equation (4.1). In the equation, μ_0 is the initial capacity in the cycle and $D(t)$ is the cumulated damage due to all clusters, $N(t)$, occurring within t.

$$\mu(t) = \mu_0 - D(t) = \mu_0 - \sum_{i=1}^{N(t)} \Delta\mu_i \tag{4.1}$$

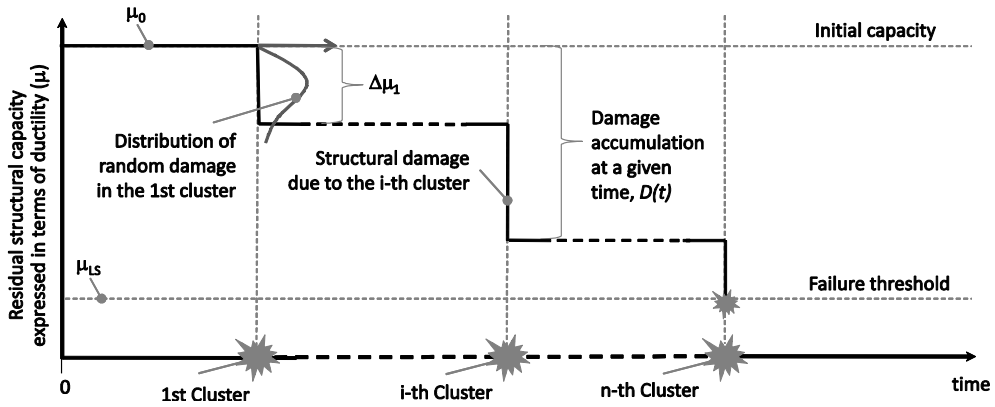

Figure 4.2. Seismic cycle representation for a structure subjected to cumulative earthquake damages.

It follows from Equation (4.1) that the probability the structure fails within time t, $P_f(t)$, that is the cumulative probability function (CDF) of structural lifetime, $F_T(t)$, complement to one of reliability, $R(t)$, is the probability that the structure passes the limit-state (LS) threshold, μ_{LS}. It can also be expressed as the probability the damage cumulated is larger than the difference between the initial capacity and the threshold, $\bar{\mu} = \mu_0 - \mu_{LS}$, as in Equation (4.2).

$$P_f(t) = F_T(t) = 1 - R(t) = P\left[\mu(t) \le \mu_{LS}\right] = P\left[D(t) \ge \mu_0 - \mu_{LS}\right] = P\left[D(t) \ge \bar{\mu}\right] \quad (4.2)$$

Because in this approach the damage in the single cluster, $\Delta\mu_i$, and $N(t)$ are both RVs, the structural reliability problem may be computed by means of the total probability theorem as in Equation (4.3), where the probability of occurrence of k clusters and the probability of failure given k clusters, appear.

$$P_f(t) = \sum_{k=1}^{+\infty} P\left[D(t) \geq \bar{\mu} \middle| N(t) = k\right] \cdot P\left[N(t) = k\right] =$$
$$= \sum_{k=1}^{+\infty} P\left[\sum_{i=1}^{k} \Delta\mu_i \geq \bar{\mu} \middle| N(t) = k\right] \cdot \frac{\left(E\left[N(t)\right]\right)^k}{k!} \cdot e^{-E\left[N(t)\right]} = \tag{4.3}$$
$$= \sum_{k=1}^{+\infty} P\left[\sum_{i=1}^{k} \Delta\mu_i \geq \bar{\mu} \middle| N(t) = k\right] \cdot \frac{(\lambda \cdot t)^k}{k!} \cdot e^{-\lambda \cdot t}$$

The equation assumes that the process regulating the occurrence of clusters is a HPP. It is an assumption directly following from classical PSHA. Indeed, if mainshock occurrence is stochastically modeled by a HPP with rate equal to λ (a common assumption in PSHA) then, the cluster initiation may be seen as described by the same process (Boyd, 2012; Iervolino et al., 2013d; Iervolino et al., 2014). Thus, $E\left[N(t)\right] = \lambda \cdot t$ is the expected number of clusters in $(0,t)$.

Once the total probability theorem is applied, and the probability of occurrence of clusters is formulated, the last issue to solve is to evaluate the probability of exceedance of a threshold for any given number of clusters, $P\left[\sum_{i=1}^{k} \Delta\mu_i \geq \bar{\mu} \mid N(t) = k\right]$.

Because the latter is the probability of the sum of damages in k individual clusters, such a probability may be easily computed if $\Delta\mu_i$, the damage in a single sequence, is modeled via a random variable that enjoys additive reproductive property.[1] It is well-know the Gaussian RV enjoys this property; however, it is not suitable to model degradation, which is a monotonic process, thus requiring damage in a single event to be a non-negative RV. On the other hand, the lognormal RV, often used in the earthquake engineering context to model non-negative random variables, is not reproductive in the (additive) sense needed in the equations above.

[1] The sum of i.i.d. RVs pertaining to a family that enjoys the reproductive property also belongs to the considered family.

Two RVs, featuring the needed property, are: the gamma (G) and the inverse-Gaussian (IG), which are two-parameters models and may be seen as particular cases of the generalized-inverse-Gaussian RV (Johnson et al., 1994). These will be considered in the following to model structural damage in earthquake clusters; however, because reproducibility requires that effects of clusters are independent, this hypothesis will be discussed in the next section along with the assumption that cluster damages are identically distributed.

4.3. Damage measures and independent and identically distributed increments hypothesis

This section focuses on the properties of damage measures that may characterize the dynamic performance of common structures in literature. According to Cosenza and Manfredi (2000) damage indices are usually comprised between two extremes: (i) *displacement-related* and (ii) *energy-related*. Measures in the former class assume that collapse is related to attainment or exceedance of some maximum strain limit. Those in the latter postulate that damage is related to the amount of energy dissipated by hysteretic loops. In fact, the most representative damage index of (i) is the maximum displacement demand, while hysteretic energy, defined as the total areas of plastic cycles during shaking, is a key member of (ii). Hybrid indices also exist (e.g., Park and Ang, 1985).

If the simplest non-linear inelastic structure is considered, that is an EPP-SDOF (Figure 4.3a), according to a displacement-based damage criterion, the accumulation of degradation occurs in the second shock, that is part of a sequence of two, only if the maximum displacement reached in the second one is larger than the maximum in the first one. This makes the damage increment dependent at least on the residual displacement of the structure at the time of the shock, and violates the hypothesis, postulated in the previous section, that the cumulative damage process has independent increments. In this case, state-dependent approaches (e.g., Yeo and Cornell, 2005; Luco et al., 2011; Giorgio et al., 2010) may be required to stochastically model degradation. On the other hand, Figure 4.3b shows that the area of hysteretic loops

during the shaking from the second shock is measured regardless of the previous shaking demand. Therefore, due to the *non-evolutionary* (Cosenza and Manfredi, 2000) features of the EPP-SDOF system response, if a damage index measuring dissipated hysteretic energy is chosen, damage increments in subsequent events are i.i.d. RVs, that is, the response of the structure to a specific shock is independent of its status prior to the shock (see section 4.4).

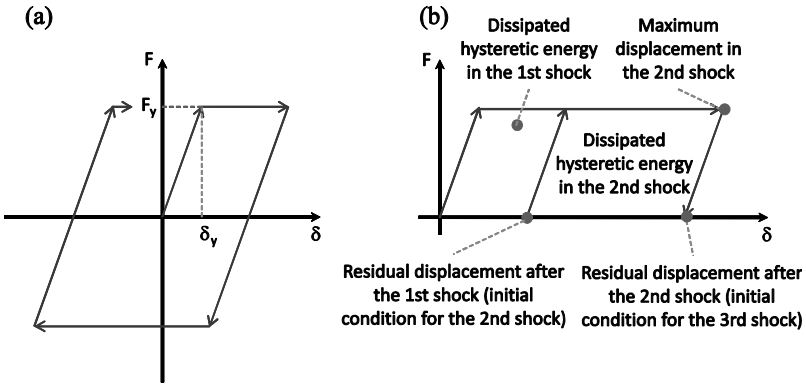

Figure 4.3. Elastic-perfectly-plastic non-evolutionary behavior (a), and monotonic (simplistic) scheme of cumulative response in terms of maximum displacement and dissipated hysteretic energy (b). F is the force, δ is the displacement, and y subscript indicates yielding.

In this study the *kinematic ductility*, μ, is considered as a simplistic proxy for dissipated hysteretic energy. It is the maximum displacement demand when the yielding displacement is the unit. To capture energy dissipation in a single shock only, ductility is computed as if the residual displacement at beginning of each ground motion is zero. Note that this implies that only events with intensity larger than that required to yield the structure may produce increment of damage. The collapse is assumed to occur when kinematic ductility, conservatively accumulated independently on the sign of maximum displacement, reaches some capacity value.

4.4. Damage distribution in the single cluster

This section targets the formulation of the distribution of damage increment in a single seismic cluster, $\Delta\mu_i$. It is the fundamental component to obtain the distribution of the sum of damage in *k* clusters as per Equation (4.3). Under the hypotheses discussed in the preceding sections, $\Delta\mu_i$ may be seen as the damage in the mainshock, $\Delta\mu_{E,i}$, plus that accumulated in the aftershock sequence, $\Delta\mu_{A,i}$, pertaining to the same mainshock, Equation (4.4).

$$\Delta\mu_i = \Delta\mu_{E,i} + \Delta\mu_{A,i} = \Delta\mu_{E,i} + \sum_{j=1}^{N_{A,i}} \Delta\mu_{A,ij} \tag{4.4}$$

In the equation, $N_{A,i}$ is the number of aftershocks in the sequence following the *i-th* mainshock and $\Delta\mu_{A,ij}$ is the damage in the *j-th* aftershock. The developed model considers all the terms of Equation (4.4) as random. Therefore, in the following it will be discussed first how $N_{A,i}$ is stochastically modeled, then the distribution of $\Delta\mu_{E,i}$ is addressed, and $\Delta\mu_{A,ij}$ is discussed. Finally the strategy for combination of these terms to get $\Delta\mu_i$ is illustrated.

4.4.1. Conditional aftershock occurrence process and APSHA hypotheses

Given the occurrence of the mainshock initiating the seismic sequence, aftershocks are modeled herein following the aftershock probabilistic seismic hazard analysis approach of Yeo and Cornell (2009a). In APSHA, assuming that the mainshock occurred at $t = 0$, the occurrence of aftershocks is described by a NHPP the daily rate of which, $\lambda_{A|M_E}$, is provided by Equation (4.5). The rate refers to the aftershocks with magnitude bounded between a minimum value of interest, $m_{\min}$, and that of the mainshock, coefficients *a* and *b* are from a suitable Gutenberg and Richter (GR) relationship

(Gutenberg and Richter, 1944), while *c* and *p* are those of the *modified Omori law* (Utsu, 1961) for the considered sequence. Therefore, the process of aftershocks may be considered conditional to the mainshock. Moreover, it follows from Equation (4.5) that the expected number of aftershocks in $(0, \Delta T_A)$ is given by Equation (4.6).

$$\lambda_{A|M_E}(t) = \left(10^{a+b\cdot(m_E - m_{\min})} - 10^{a}\right) \Big/ (t+c)^{p} \tag{4.5}$$

$$\begin{aligned} &E\left[N_A(\Delta T_A)\middle| M_E = x\right] = \\ &= \int_0^{\Delta T_A} \lambda_{A|M_E}(\tau)\cdot d\tau = \frac{10^{a+b\cdot(m_E - m_{\min})} - 10^{a}}{p-1} \cdot \left[c^{1-p} - (\Delta T_A + c)^{1-p}\right] \end{aligned} \tag{4.6}$$

APSHA, provides the rate of exceedance of a ground motion intensity measure (*IM*) at a site of interest, $\lambda_{IM_A|M_E,R_E}(t)$, during the aftershock sequence, via Equation (4.7).

$$\begin{aligned} &\lambda_{IM_A|M_E,R_E}(t) = \\ &= \lambda_{A|M_E}(t) \cdot \int_{r_A}\int_{m_A} P\left[IM > im \middle| M_A = w, R_A = z\right] \cdot f_{M_A,R_A|M_E,R_E}(w,z|x,y)\cdot dw \cdot dz \end{aligned} \tag{4.7}$$

In the equation, $f_{M_A,R_A|M_E,R_E}$ is the distribution of the aftershock magnitude and distance, $\{M_A, R_A\}$, conditional to those of the mainshock, $\{M_E, R_E\}$,[2] while $P\left[IM > im \middle| M_A = w, R_A = z\right]$ is the probability of exceedance of *IM* conditional to magnitude and distance from a ground motion prediction equation (GMPE). It is worth to note that, to obtain Equation (4.7), APSHA also assumes that *IMs* in different aftershocks are i.i.d., given $\{M_E, R_E\}$.

[2] This factually makes the aftershock rate to be dependent also on location of the mainshock and not only on magnitude.

4.4.2. Mainshock damage

The PDF of the first term at the right hand side of Equation (4.4) that is the damage in the mainshock, $\Delta\mu_{E,i}$, is computed consistently with PBEE. Indeed, the distribution of $\Delta\mu_{E,i}$, $f_{\Delta\mu_{E,i}}(\delta\mu)$, is calculated as in Equation (4.8).

$$f_{\Delta\mu_{E,i}}(\delta\mu) = \int_{im} f_{\Delta\mu_{E,i}|IM}(\delta\mu|u)\cdot f_{IM_E}(u)\cdot du = \\ = \int_{im} f_{\Delta\mu_{E,i}|IM}(\delta\mu|u)\cdot \int_{r_E}\int_{m_E} f_{IM|M_E,R_E}(u|x,y)\cdot f_{M_E,R_E}(x,y)\cdot dx\cdot dy\cdot du \tag{4.8}$$

In the equation $f_{\Delta\mu_{E,i}|IM}$ is the distribution of damage given an *IM* value (e.g., from incremental dynamic analysis or IDA; Vamvatsikos and Cornell, 2002), while f_{IM_E} is the PDF of the chosen *IM* given the occurrence of a mainshock. Indeed, as per the right hand side of Equation (4.8), the latter can be computed as in PSHA, via the joint PDF of mainshock magnitude and distance RVs for the site of the construction, f_{M_E,R_E}, and the distribution of *IM* given the mainshock parameters, $f_{IM|M_E,R_E}$, provided by a GMPE. In the case $\{M_E,R_E\}$ may be considered stochastically independent, the joint PDF is just the product of the marginal distribution of magnitude, often described by a GR relationship, and that of source-to-site distance, which depends on the source-site geometrical configuration. In fact, it will be shown in section 4..4.4 that to compute the distribution in the cluster, the distribution of damage in the mainshock, conditional to $\{M_E,R_E\}$ is of interest. It follows from Equation (4.8) and is given in Equation (4.9) in the case the structural response is independent of $\{M_E,R_E\}$ given *IM*.

$$f_{\Delta\mu_{E,i}|M_E,R_E}(\delta\mu|x,y) = \int_{im} f_{\Delta\mu_{E,i}|IM}(\delta\mu|u)\cdot f_{IM|M_E,R_E}(u|x,y)\cdot du \tag{4.9}$$

4.4.3. Damage in the generic aftershock given the mainshock

To compute the distribution of damage in the single aftershock of a certain mainshock, a similar approach can be used, as depicted in Equation (4.10). In the equation, $f_{IM_A|M_E,R_E}$ is the distribution of the ground motion intensity given the occurrence of a mainshock of magnitude $M_E = x$ and separated by a distance $R_E = y$ from the site; i.e., from APSHA.[3] In fact, $f_{IM_A|M_E,R_E}$ is the PDF corresponding to the integral term of Equation (4.7).

$$\begin{aligned} f_{\Delta\mu_{A,ij}|M_E,R_E}\left(\delta\mu|x,y\right) &= \int_{im} f_{\Delta\mu_{A,ij}|IM}\left(\delta\mu|u\right)\cdot f_{IM_A|M_E,R_E}\left(u|x,y\right)\cdot du = \\ &= \int_{im} f_{\Delta\mu_{A,ij}|IM}\left(\delta\mu|u\right)\cdot \int_{r_A}\int_{m_A} f_{IM|M_A,R_A}\left(u|w,z\right)\cdot f_{M_A,R_A|M_E,R_E}\left(w,z|x,y\right)\cdot dw\cdot dz\cdot du \end{aligned} \tag{4.10}$$

Note that the $f_{\Delta\mu_{A,ij}|IM}$ term is the same as $f_{\Delta\mu_{E,i}|IM}$ in Equation (4.9). Indeed, in both equations it is assumed that the response of the structure is, given the *IM*, the same in mainshock and one aftershock, $f_{\Delta\mu_{E,i}|IM} = f_{\Delta\mu_{A,ij}|IM}$, and independent on specific features of the earthquake (see section 4.6). In this case, the *IM* is said to be a *sufficient* one (Luco and Cornell, 2007). Moreover, it is also assumed that the same GMPE can be

[3] Models used in this study consider that the aftershock source zone depends on the magnitude and location of the mainshock. Considering magnitude and distance, instead, is equivalent herein. It is also to note that both $f_{IM_A|M_E,R_E}$ and $f_{IM_E|M_E,R_E}$ should be indicated as $f_{IM_{A,ij}|M_E,R_E}$ and $f_{IM_{E,i}|M_E,R_E}$, yet the notation is intentionally simplified due to the i.i.d. features of these RVs. Actually, while also damages are i.i.d., subscript are kept there to avoid confusion, as it will be clarified in the following.

used for both mainshock and aftershocks, so also the $f_{IM|M_A,R_A}$ term is the same as $f_{IM|M_E,R_E}$.

4.4.4. Cluster damage

On the basis of the above equations, it is possible to approach the distribution of damage in the whole cluster. Recalling Equation (4.4), the probability of exceedance of any damage level can be computed as in Equation (4.11).

$$\begin{aligned} &P\left[\Delta\mu_i > \delta\mu\right] = P\left[\Delta\mu_{E,i} + \Delta\mu_{A,i} > \delta\mu\right] = \\ &= 1 - P\left[\Delta\mu_{E,i} + \Delta\mu_{A,i} \le \delta\mu\right] = 1 - P\left[\Delta\mu_{E,i} + \sum_{j=1}^{N_{A,i}(\Delta T_A)} \Delta\mu_{A,ij} \le \delta\mu\right] \end{aligned} \tag{4.11}$$

Because of the features of the EPP-SDOF response introduced in section 4.3, it may be argued that conditional to $\{M_E, R_E\}$, the increment damage in the mainshock and in the aftershock sequence are independent random variables. This is because, as discussed in section 4.2, the damage from any single event in a cluster only depends on the *IM*; moreover, the *IMs* associate to the events in a cluster are independent given the features of the triggering mainshock. Hence, applying the total probability theorem, $P\left[\Delta\mu_{E,i} + \Delta\mu_{A,i} \le \delta\mu\right]$ of Equation (4.11) can be rewritten as in Equation (4.12).

$$\begin{aligned} &P\left[\Delta\mu_{E,i} + \Delta\mu_{A,i} \le \delta\mu\right] = \\ &= \int_{r_E}\int_{m_E} P\left[\Delta\mu_i \le \delta\mu \middle| M_E = x, R_E = y\right] \cdot f_{M_E,R_E}(x,y) \cdot dx \cdot dy = \\ &= \int_{r_E}\int_{m_E}\int_{0}^{\delta\mu} P\left[\Delta\mu_{E,i} \le \delta\mu - l \middle| M_E = x, R_E = y\right] \cdot f_{\Delta\mu_{A,i}|M_E,R_E}(l|x,y) \cdot f_{M_E,R_E}(x,y) \cdot dl \cdot dx \cdot dy \end{aligned} \tag{4.12}$$

In the above equation, the term $P\left[\Delta\mu_{E,i} \le \delta\mu - l \,|\, M_E = x, R_E = y\right]$ is obtained from Equation (4.9), while $f_{\Delta\mu_{A,i}|M_E,R_E}$ represents the PDF of damage cumulated during the

aftershock sequence, given the features of the mainshock. Because, as discussed, the aftershock sequence is comprised by a random number of events, $f_{\Delta\mu_{A,i}|M_E,R_E}$ can be evaluated applying the total probability theorem again; Equation (4.13). Note that, following the APSHA approach, the probability of having j aftershocks in the cluster is provided by a Poisson distribution with mean in Equation (4.6). In the equation it is assumed that $f_{\Delta\mu_{A,i}|M_E,R_E,N_{A,i}}$ degenerates in a unitary mass at zero when *j* equals zero.

$$\begin{aligned} f_{\Delta\mu_{A,i}|M_E,R_E}\left(l|x,y\right) &= \sum_{j=0}^{+\infty} f_{\Delta\mu_{A,i}|M_E,R_E,N_{A,i}}\left(l|x,y,j\right)\cdot P\left[N_{A,i}\left(\Delta T_A\right)=j|M_E=x\right]= \\ &= \sum_{j=0}^{+\infty} f_{\Delta\mu_{A,i}|M_E,R_E,N_{A,i}}\left(l|x,y,j\right)\cdot\frac{\left(E\left[N_{A,i}\left(\Delta T_A\right)|M_E=x\right]\right)^j}{j!}\cdot e^{-E\left[N_{A,i}(\Delta T_A)|M_E=x\right]} \end{aligned} \tag{4.13}$$

Under the assumption that damages produced in different aftershock events are i.i.d. RVs, given $\{M_E,R_E\}$, which follows from sections 4.3 and 4.2, the distribution of the sum of damages in a given number of aftershocks, conditional to magnitude and distance of the mainshock, $f_{\Delta\mu_{A,i}|M_E,R_E,N_{A,i}}$, is just the *j-th* order convolution of $f_{\Delta\mu_{A,ij}|M_E,R_E}$ from Equation (4.10), with itself, and it will be indicated as $f^{(j)}_{\Delta\mu_{A,i}|M_E,R_E}$ in the following.

Applying a further simplification of the delta method (e.g., Oehlert, 1992) to Equation (4.13), the infinite-terms summation may be approximated by the term corresponding to the expected number of aftershocks in the time interval of interest, Equation (4.14).

$$\begin{cases} f_{\Delta\mu_{A,i}|M_E,R_E}\left(l|x,y\right) = \\ = \sum_{j=0}^{+\infty} f^{(j)}_{\Delta\mu_{A,ij}|M_E,R_E}\left(l|x,y\right)\cdot \dfrac{\left(E\left[N_{A,i}\left(\Delta T_A\right)|M_E=x\right]\right)^j}{j!}\cdot e^{-E\left[N_{A,i}\left(\Delta T_A\right)|M_E=x\right]} \approx \\ \approx f^{(\tilde{N}_A)}_{\Delta\mu_{A,ij}|M_E,R_E}\left(l\,|\,x,y\right) \\ \tilde{N}_A = \mathrm{int}\left\{E\left[N_{A,i}\left(\Delta T_A\right)|M_E=x\right]\right\} = \int_t^{\Delta T_A} \lambda_{A|m_E=x}\left(\tau\right)\cdot d\tau \end{cases} \tag{4.14}$$

At this point, combining Equation (4.14) with Equation (4.12), the probability of exceedance of an increment damage value in the single cluster results, and it is given in Equation (4.15), where it is assumed that $f^{(\tilde{N}_A)}_{\Delta\mu_{A,ij}|M_E,R_E}$ degenerates in a unitary probability mass at $\delta\mu_{A,ij}=0$ when $\tilde{N}_A=0$.[4]

$$\begin{aligned} &P\left[\Delta\mu_i > \delta\mu\right] = \\ &= 1-\int_{r_E}\int_{m_E}\int_0^{\delta\mu} P\left[\Delta\mu_{E,i} \le \delta\mu - l\,|M_E=x, R_E=y\right]\cdot f^{(\tilde{N}_A)}_{\Delta\mu_{A,ij}|M_E,R_E}\left(l|x,y\right)\cdot f_{M_E,R_E}\left(x,y\right)\cdot dl\cdot dx\cdot dy \end{aligned} \tag{4.15}$$

The strategy to compute the integral in Equation (4.15) will be discussed in section 4.6, while section 4.5 introduces the advantage of assuming that $\Delta\mu_i$ follows a G or an IG distribution.

[4] In Equation (4.15), and in others above, the distribution of damage is always indicated as a PDF, for simplicity of notation. However, it is not perfectly appropriate because the damage in a single event is not a continuous RV, as it will be clarified in the application.

4.5. Reliability solutions for Gamma and Inverse Gaussian damage in the cluster

Because the EPP-SDOF assures the RVs adopted to model damages, $\Delta\mu_i$, accumulated over different clusters are i.i.d., a closed-form solution of the reliability problem may be obtained if the sum of the damages in multiple mainshock-aftershock sequences may be expressed using a (non-negative) RV, which possesses the reproductive property.

4.5.1. Gamma-distributed damage increments

An option discussed in Iervolino et al. (2013a) is given in Equation (4.16), in which it is considered that the damage increment is a gamma-distributed RV (Γ is the gamma function). The PDF of this RV is indexed by two parameters, γ_D and α_D, the scale and shape parameters, respectively. The mean and variance are α_D/γ_D and α_D/γ_D^2 respectively.

$$f_{\Delta\mu_i}(\delta\mu)=\frac{\gamma_D\cdot(\gamma_D\cdot\delta\mu)^{\alpha_D-1}}{\Gamma(\alpha_D)}\cdot e^{-\gamma_D\cdot\delta\mu} \tag{4.16}$$

The main advantage in using the gamma model in the context of this study is that the sum of k_D i.i.d. G-distributed RVs, with scale and shape parameters γ_D and α_D, is still G-distributed with parameters γ_D and $k_D\cdot\alpha_D$. Therefore, the probability of cumulative damage exceeding the threshold, conditional to k_D shocks, is given by Equation (4.17) where $\Gamma(k_D\cdot\alpha_D)$ and $\Gamma_U(k_D\cdot\alpha_D,\gamma_D\cdot\bar{\mu})$ are referred to as the *incomplete* and the *upper-incomplete* gamma functions, respectively.

$$P\left[D(t)\geq\bar{\mu}\,\middle|\,N_D(t)=k_D\right]=\int_{\bar{\mu}}^{+\infty}\frac{\gamma_D(\gamma_D\cdot x)^{k_D\cdot\alpha_D-1}}{\Gamma(k_D\cdot\alpha_D)}\cdot e^{-\gamma_D\cdot x}\cdot dx=\frac{\Gamma_U(k_D\cdot\alpha_D,\gamma_D\cdot\bar{\mu})}{\Gamma(k_D\cdot\alpha_D)} \tag{4.17}$$

Equation (4.17), allows a closed-form solution of the reliability problem given in Equation (4.3). However, because the gamma is a continuous RV, it gives $P\left[\Delta\mu_i = 0\right] = 0$, thus, it can be adopted to account only for the effects of damaging clusters (this justifies the subscript *D*). This is the reason why the rate in Equation (4.3) has to be the one referring to damaging sequences, which can be obtained as the *total* cluster rate, λ, times the probability that a cluster is damaging, that is $\lambda_D = \lambda \cdot P\left[\Delta\mu_i > 0\right]$.

That said, it might be worth to introduce an approximation enabling closed-form for the reliability assessment. This is given in Equation (4.18) where $P_f(t)$ is replaced by the probability conditional to the expected number of damaging clusters until t. Tolerability of this approximation will be discussed in the application section.

$$
\begin{aligned}
P_f(t) &= \sum_{k_D=1}^{+\infty} P\left[D(t) \geq \bar{\mu} \middle| N_D(t) = k_D \right] \cdot \frac{(\lambda_D \cdot t)^{k_D}}{k_D!} \cdot e^{-\lambda_D \cdot t} = \\
&= \sum_{k_D=1}^{+\infty} P\left[\sum_{i=1}^{k_D} \Delta\mu_i \geq \bar{\mu} \middle| N_D(t) = k_D \right] \cdot \frac{(\lambda_D \cdot t)^{k_D}}{k_D!} \cdot e^{-\lambda_D \cdot t} \approx \\
&= P\left[D(t) \geq \bar{\mu} \middle| N_D(t) = E\left[N_D(t)\right] \right] = P\left[D(t) \geq \bar{\mu} \middle| N_D(t) = \lambda_D \cdot t \right] = \\
&= \frac{\Gamma_U\left(\lambda_D \cdot t \cdot \alpha_D, \gamma_D \cdot \bar{\mu}\right)}{\Gamma\left(\lambda_D \cdot t \cdot \alpha_D\right)}
\end{aligned}
\tag{4.18}
$$

4.5.2. Inverse-Gaussian-distributed damage increments

Another RV with similar properties as those of the gamma, is the inverse-Gaussian, Equation (4.19). The IG distribution is the well-known solution of the first-passage time problem in processes regulated by Brownian motions (e.g., Matthews et al., 2002). Also this RV has a PDF that is indexed by two parameters: η_D and ν_D. The mean and variance are ν_D and ν_D / η_D^3 respectively.

$$f_{\Delta\mu_i}(\delta\mu) = \sqrt{\frac{\eta_D}{2\cdot\pi\cdot\delta\mu^3}}\cdot e^{-\frac{\eta_D\cdot(\delta\mu-\nu_D)^2}{2\cdot\nu_D^2\cdot\delta\mu}} \tag{4.19}$$

The sum of k_D i.i.d. IG-distributed RVs, each of which with parameters η_D and ν_D, is still IG with parameters $k_D^2\cdot\eta_D$ and $k_D\cdot\nu_D$; see Equation (4.20), where F_{IG} is the CDF of the IG-RV.
Therefore, following from Equation (4.18), the failure probability in Equation (4.3) can be approximated by Equation (4.21).

$$P\left[D(t)\geq\bar{\mu}\middle|N_D(t)=k_D\right] = \int_{\bar{\mu}}^{+\infty}\sqrt{\frac{k_D^2\cdot\eta_D}{2\cdot\pi\cdot x^3}}\cdot e^{-\frac{\eta_D\cdot(x-k_D\cdot\nu_D)^2}{2\cdot\nu_D^2\cdot x}}\cdot dx = \\ = 1-F_{IG}\left(\bar{\mu};k_D{}^2\cdot\eta_D,k_D\cdot\nu_D\right) \tag{4.20}$$

$$P_f(t)\approx P\left[D(t)\geq\bar{\mu}\middle|N_D(t)=E\left[N_D(t)\right]\right]=1-F_{IG}\left(\bar{\mu};\lambda_D^2\cdot t^2\cdot\eta_D,\lambda_D\cdot t\cdot\nu_D\right) \tag{4.21}$$

4.5.3. Conditional reliability approximations

Formulations above provide the absolute (i.e., aprioristic) probability that a new structure fails in a time interval of interest $(0,t)$. However, according to the formulated models, it is possible to include in the reliability assessment other information about the structural conditions (e.g., after an inspection), still retaining the closed-forms (Iervolino et al. 2013a-b). In particular, it is possible to formulate the conditional failure probabilities when: (1) the residual capacity of the structure is known at the time of the reliability assessment; (2) it is only known that the structure is above the failure threshold at the time the evaluation is performed, yet with unknown residual seismic capacity; (3) same of case (2) with the additional information of the number of damaging clusters the structure suffered up to the time of the assessment.
(1) In this case, at t^* during the life-cycle, the present capacity, $\mu(t^*)$, of the structure is measured. The failure probability conditional to observed state has the same

expression above, just, replacing $\bar{\mu}$ and t of Equations (4.18) and (4.21), with $\bar{\mu}^* = \mu\left(t^*\right) - \mu_{LS}$ and $t - t^*$. In fact, the structure has now to undergo a smaller capacity reduction to fail. Equation (4.22) and Equation (4.23) provide such probability when the damage increment in the cluster is susceptible of G or IG representation, respectively.[5]

$$P\left[D(t) \geq \bar{\mu} \left| \mu\left(t^*\right) - \mu_{LS} = \bar{\mu}^* \right. \right] \approx \frac{\Gamma_U\left[\lambda_D \cdot \left(t - t^*\right) \cdot \alpha_D, \gamma_D \cdot \bar{\mu}^* \right]}{\Gamma\left[\lambda_D \cdot \left(t - t^*\right) \cdot \alpha_D \right]}, \; t > t^* \tag{4.22}$$

$$\begin{aligned} &P\left[D(t) \geq \bar{\mu} \left| \mu\left(t^*\right) - \mu_{LS} = \bar{\mu}^* \right. \right] \approx \\ &\approx 1 - F_{IG}\left[\bar{\mu}^*; \lambda_D^2 \cdot \left(t - t^*\right)^2 \cdot \eta_D, \lambda_D \cdot \left(t - t^*\right) \cdot \nu_D \right], \quad t > t^* \end{aligned} \tag{4.23}$$

(2) The second case considers that at t^* the structure is still surviving but with unknown damage condition. Failure probability may be computed via Equation (4.24) and it specializes in Equation (4.25) and Equation (4.26) for G and IG cases, respectively.

$$\begin{aligned} &P\left[D(t) \geq \bar{\mu} \left| \mu\left(t^*\right) > \mu_{LS} \right. \right] = 1 - P\left[D(t) < \bar{\mu} \left| \mu\left(t^*\right) > \mu_{LS} \right. \right] = \\ &= 1 - \frac{P\left[D(t) < \bar{\mu} \cap \mu\left(t^*\right) > \mu_{LS} \right]}{P\left[\mu\left(t^*\right) > \mu_{LS} \right]} = 1 - \frac{R(t)}{R\left(t^*\right)} = 1 - \frac{1 - P_f(t)}{1 - P_f\left(t^*\right)}, \quad t > t^* \end{aligned} \tag{4.24}$$

[5] The same relationship may be also used if the residual capacity $\bar{\mu}^*$ is obtained via a repair at t^*.

$$P\left[D(t) \geq \bar{\mu} \middle| \mu(t^*) > \mu_{LS} \right] \approx 1 - \frac{1 - \dfrac{\Gamma_U\left[\lambda_D \cdot t \cdot \alpha_D, \gamma_D \cdot \bar{\mu}\right]}{\Gamma\left[\lambda_D \cdot t \cdot \alpha_D\right]}}{1 - \dfrac{\Gamma_U\left[\lambda_D \cdot t^* \cdot \alpha_D, \gamma_D \cdot \bar{\mu}\right]}{\Gamma\left[\lambda_D \cdot t^* \cdot \alpha_D\right]}}, \quad t > t^* \tag{4.25}$$

$$P\left[D(t) \geq \bar{\mu} \middle| \mu(t^*) > \mu_{LS} \right] \approx 1 - \frac{F_{IG}\left(\bar{\mu}; \lambda_D^2 \cdot t^2 \cdot \eta_D, \lambda_D \cdot t \cdot \nu_D\right)}{F_{IG}\left[\bar{\mu}; \lambda_D^2 \cdot (t^*)^2 \cdot \eta_D, \lambda_D \cdot t^* \cdot \nu_D\right]}, \quad t > t^* \tag{4.26}$$

(3) Finally, Equation (4.27) provides the probability of failure given the structure surviving at time t^* after $N_D(t^*) = k_D$ damaging clusters. Equation (4.28) and Equation (4.29) specialize for the G and IG cases, respectively.

$$\begin{aligned} P\left[D(t) \geq \bar{\mu} \middle| \mu(t^*) > \mu_{LS} \cap N_D(t^*) = k_D \right] &= 1 - \frac{1 - P\left[\sum_{i=1}^{k_D + N_D(t - t^*)} \Delta\mu_i \geq \bar{\mu}\right]}{1 - P\left[\sum_{i=1}^{k_D} \Delta\mu_i \geq \bar{\mu}\right]} = \\ &= 1 - \frac{1 - \sum_{k_D^*=0}^{+\infty} P\left[\sum_{i=1}^{k_D + k_D^*} \Delta\mu_i \geq \bar{\mu} \middle| N_D(t - t^*) = k_D^*\right] \cdot P\left[N_D(t - t^*) = k_D^*\right]}{1 - P\left[\sum_{i=1}^{k_D} \Delta\mu_i \geq \bar{\mu}\right]}, \quad t > t^* \end{aligned} \tag{4.27}$$

$$P\left[D(t) \geq \bar{\mu} \middle| \mu(t^*) > \mu_{LS} \cap N_D(t^*) = k_D \right] \approx \tag{4.28}$$

$$\approx 1 - \frac{1 - \dfrac{\Gamma_U\left[k_D \cdot \alpha_D + \lambda_D \cdot (t - t^*) \cdot \alpha_D, \gamma_D \cdot \bar{\mu}\right]}{\Gamma\left[k_D \cdot \alpha_D + \lambda_D \cdot (t - t^*) \cdot \alpha_D\right]}}{1 - \dfrac{\Gamma_U\left[k_D \cdot \alpha_D, \gamma_D \cdot \bar{\mu}\right]}{\Gamma\left[k_D \cdot \alpha_D\right]}}, \quad t > t^*$$

$$P\left[D(t) \geq \bar{\mu} \middle| \mu(t^*) > \mu_{LS} \cap N_D(t^*) = k_D \right] \approx$$

$$\approx 1 - \frac{F_{IG}\left\{ \bar{\mu}; \left[k_D + \lambda_D \cdot (t - t^*) \right]^2 \cdot \eta_D, \left[k_D + \lambda_D \cdot (t - t^*) \right] \cdot \nu_D \right\}}{F_{IG}\left(\bar{\mu}; k_D^2 \cdot \eta_D, k_D \cdot \nu_D \right)}, \quad t > t^* \tag{4.29}$$

4.6. Model calibration strategy via an illustrative application

To evaluate the developed models, an ideal application is performed. To this aim a simple EPP-SDOF system with unloading/reloading stiffness always equal to initial one, is considered. The period of the SDOF system is assumed to be equal to 0.5 s, its weight is 100 kN and the yielding force is equal to 10 kN, viscous damping is set at 5%. The following sub-sections first illustrate the calibration of the damage cluster model. Then, the results of the reliability assessment are discussed. Finally, a comparison with the case the effect of aftershocks is neglected is carried out.

4.6.1. Mainshock and aftershock intensity distributions

The structure was assumed to be within a generic seismogenic source zone, the size of which is $20 \times 80\, km^2$. Mainshock epicenters were assumed as uniformly distributed in the source zone discretized by means of the lattice depicted in Figure 4.4. The event rate of mainshocks, and then of clusters, was arbitrarily, assumed to be $\lambda = 0.013 \left[events/yr \right]$. The magnitude distribution of mainshocks was taken as a truncated exponential defined in the $[5, 6.5]$ range. The *b*-value of the GR relationship was set to 1.056; $\{M_E, R_E\}$ were considered independent RVs. It was assumed that each mainshock has its aftershocks constrained in an area around its epicenter. The size of the aftershock seismogenic zone in squared kilometers, S_A, depends on the triggering event's magnitude according to Equation (4.30) from Utsu (1970). Within

this area, arbitrarily assumed to be a square, epicenters are uniformly distributed on a lattice with 0.5 km spacing (see Iervolino et al., 2014, for a discussion related to these issues).

$$S_A = 10^{(m_E - 4.1)} \tag{4.30}$$

The length of aftershock sequences (ΔT_A) is set to 90 days after the mainshock (following Yeo and Cornell, 2009a). The parameters appearing in Equation (4.5), were: $a = -1.66, b = 0.96$, $c = 0.03$, $p = 0.93$, and $m_{\min} = 4.5$; i.e., those of generic aftershock sequences in Italy according to Lolli and Gasperini (2003).

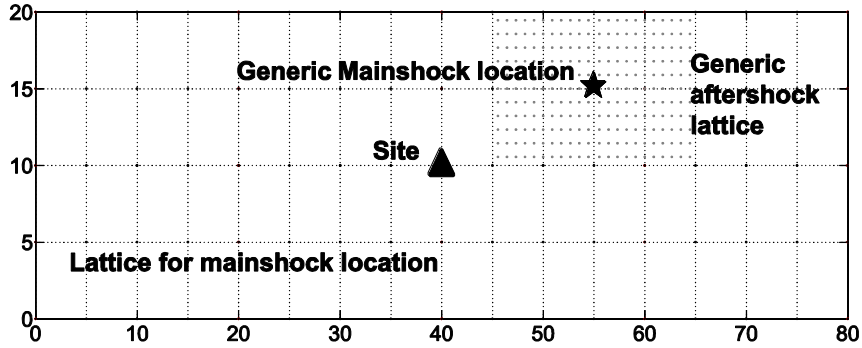

Figure 4.4. Seismogenic source lattice for mainshocks, generic aftershock lattice around a mainshock epicenter, and site.

Given this set of parameters and source models, the distributions of *IM*, in the mainshock and in the generic aftershock, given magnitude and location of the mainshock, were computed via the integrals over magnitude and distance appearing at the right hand sides of Equation (4.8) and Equation (4.10).[6]

[6] In fact, they are hazard integrals where the rate is not considered as these PDF are *given* the occurrence of the event of interest.

As an example, Figure 4.5 reports these distributions for some values representing the mainshock features.

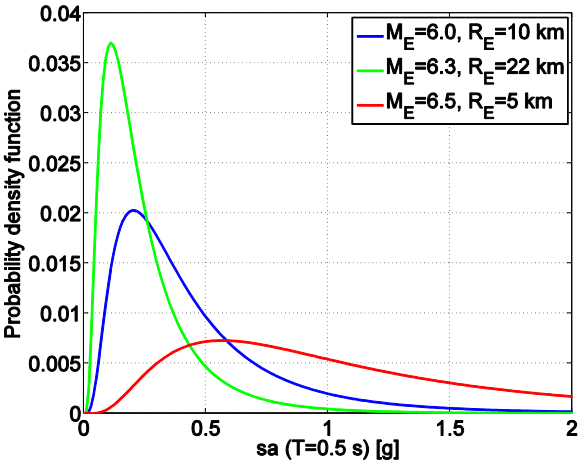

Figure 4.5. Distribution of IM in the mainshock given its features.

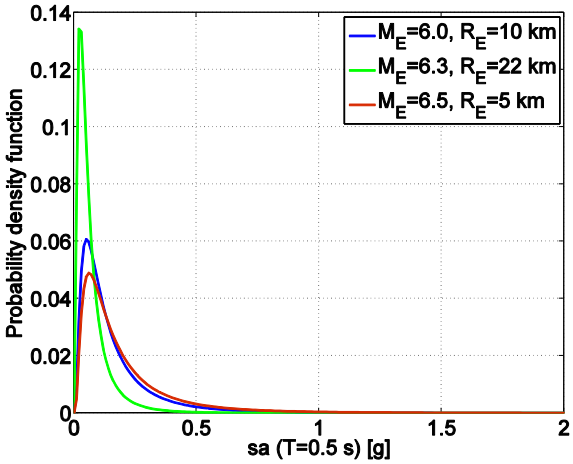

Figure 4.6. Distribution of IM in the generic aftershock given the features of the mainshocks as per APSHA.

The required $f_{IM|M_E,R_E}$ and $f_{IM|M_A,R_A}$ terms for these calculations were taken considering the Ambraseys et al. (1996) GMPE, on rock sites, converting the epicentral distance, to R_{jb} distance (Joyner and Boore 1981) used by this GMPE, via a semi-empirical relationship (Gruppo di Lavoro, 2004).

4.6.2. Distribution of damage given intensity of single earthquake shock

As discussed in section 4.3, the parameter chosen as a proxy for dissipating hysteretic energy in a single earthquake is the kinematic ductility computed as if the residual displacement of the structure before the earthquake was zero. Hence, the damage increment, $\Delta\mu$, in each earthquake event may be evaluated via Equation (4.31).

$$\Delta\mu = \frac{\delta_{\max} - \delta_y}{\bar{\delta} - \delta_y} = \frac{\mu}{\mu_0} \tag{4.31}$$

In the equation $\delta_{\max}$ is the maximum absolute value of plastic displacement demand and $\bar{\delta}$ is the displacement associated to the ductility capacity; recalling that μ_0 is the initial capacity, values of $\Delta\mu$ larger than one imply failure. Moreover, as discussed, damage is zero in those shocks not able to push the structure beyond yielding, which means ground motions with 5% damped spectral acceleration at 0.5 s lower than 0.10 g. Because the response of the considered structure in terms of hysteretic energy in a generic earthquake shock should have always the same distribution given a sufficient *IM* – e.g., first mode spectral acceleration at the elastic period of the SDOF, or $Sa(T)$ – and it is independent on the shaking history, then a single set of IDAs is sufficient to calibrate the damage distribution conditional to earthquake intensity, $f_{\Delta\mu|IM}$. In particular, it is sufficient to analyze the response of the as-new structure (see also Iervolino et al., 2013a-c). To this aim, IDAs have been performed using 30 records selected via REXEL (Iervolino et al., 2010), with moment magnitude between 5 and 7,

epicentral distances lower than 30 km and stiff site class;[7] Figure 4.7 shows IDA's output. For $f_{\Delta\mu|IM}$ a lognormal distribution was assumed, as well-established hypothesis in the PBEE context. Figure 4.8 shows some of these conditional PDFs.

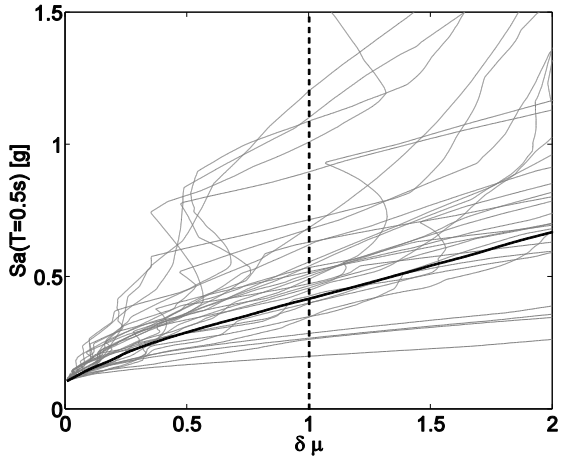

Figure 4.7. Ductility demand from IDAs.

[7] The same records and analyses have been used to calculate the response of the structure to aftershocks.

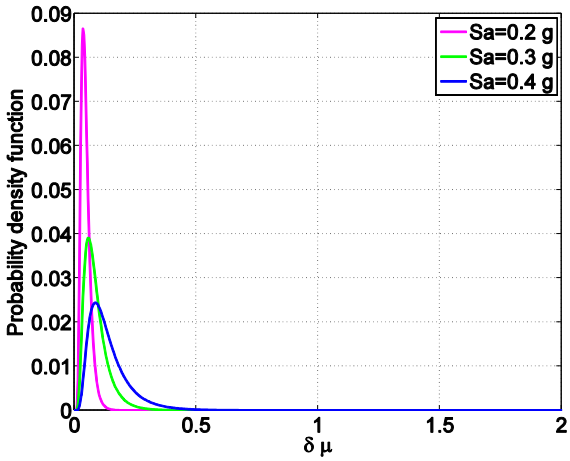

Figure 4.8. Some distributions of damage conditional to ground motion intensity.

4.6.3. Damage distributions in mainshock, in the aftershock sequence, and in the cluster

The integration of the distributions as per sections 4.5.1 and 4.5.2 allowed to get the PDFs of damage in the mainshocks and in a generic aftershock conditional to any value of the magnitude and distance of the mainshock, according to Equation (4.9) and Equation (4.10); as an example, some $f_{\Delta\mu_{E,i}|M_E,R_E}$ and $f_{\Delta\mu_{A,ij}|M_E,R_E}$ distributions are given in Figures 4.9 and 4.10. Note that, even if not represented in the figure, both these functions have a concentrated mass at zero, which is the probability that the earthquake of interest is not damaging. Indeed, due to the damage criterion considered, only the shocks with intensity larger than that causing yielding of the SDOF are able to induce hysteretic dissipation in the structure, then damage.

In analytical terms, these distributions are defined as in Equation (4.32) and in Equation (4.33). In the cases of Figures 4.9 and 4.10 $P^0_{E,i|M_E,R_E}=\{0.27,0.08,0.22\}$ for $\{M_E=6.5,R_E=5\}$, $\{M_E=6.0,R_E=10\}$, $\{M_E=6.3,R_E=22\}$, respectively, while $P^0_{A,ij|M_E,R_E}=\{0.39,0.48,0.81\}$ for $\{M_E=6.5,R_E=5\}$, $\{M_E=6.0,R_E=10\}$,

$\{M_E = 6.3, R_E = 22\}$, respectively (these probability masses are not shown in the pictures because of scale issues).

$$P\left[\Delta\mu_{E,i|M_E,R_E} \le \delta\mu\right] = \begin{cases} P^0_{E,i|M_E,R_E}(x,y) & \delta\mu = 0 \\ P^0_{E,i|M_E,R_E} + \int_0^{\delta\mu} f_{\Delta\mu_{E,i}|M_E,R_E}(z|x,y)\cdot dz & \delta\mu > 0 \end{cases} \quad (4.32)$$

$$P\left[\Delta\mu_{A,ij|M_E,R_E} \le \delta\mu\right] = \begin{cases} P^0_{A,ij|M_E,R_E}(x,y) & \delta\mu = 0 \\ P^0_{A,ij|M_E,R_E} + \int_0^{\delta\mu} f_{\Delta\mu_{A,ij}|M_E,R_E}(z|x,y)\cdot dz & \delta\mu > 0 \end{cases} \quad (4.33)$$

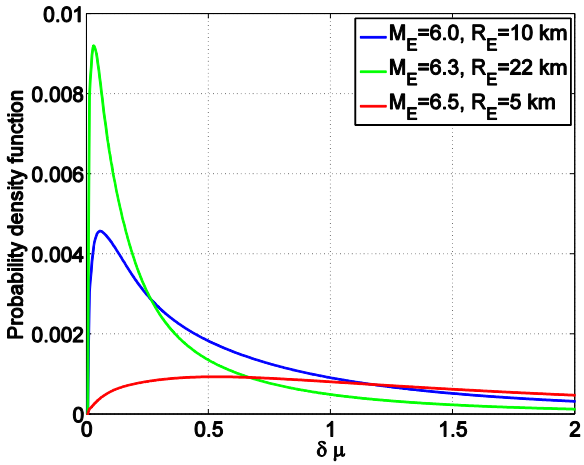

Figure 4.9. Distribution of damage in the mainshock conditional to some magnitude and distance values.

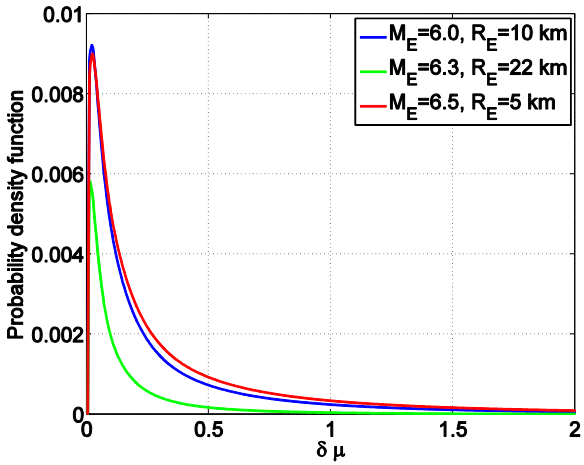

Figure 4.10. Distribution of damage in in the generic aftershock conditional to the same features of the mainshock.

It is to recall now that, while $f_{\Delta\mu_{E,i}|M_E,R_E}$ is directly needed to compute the damage in the cluster as per Equation (4.15), $f^{(\tilde{N}_A)}_{\Delta\mu_{A,ij}|M_E,R_E}$ is required for aftershocks. As discussed, it is the PDF of the sum of damage in the aftershocks sequence conditional to a $\{M_E, R_E\}$ mainshock, when the expected number $(\tilde{N}_A)$ of aftershocks in ΔT_A occurs. It is convenient here to refer to the process counting the number damaging aftershocks, as they are the only contributing to damage accumulation. Because of the properties of Poisson processes, the rate of damaging aftershocks is simply that in Equation (4.5) times the probability that an aftershock is damaging, Equation (4.34). The integer part of the expected number of damaging aftershocks is then termed $\tilde{N}_{A,D}$.

$$\lambda_{A,D|M_E,R_E} = \lambda_{A|M_E}(t)\cdot P\left[\Delta\mu_{A,ij|M_E,R_E} > 0\right] = \lambda_{A|M_E}(t)\cdot\left(1-P^0_{A,ij|M_E,R_E}\right) \tag{4.34}$$

Because, given $\{M_E, R_E\}$, damage in different aftershocks are i.i.d., $f^{(\tilde{N}_{A,D})}_{\Delta\mu_{A,ij}|M_E,R_E}$ is just the convolution of $f_{\Delta\mu_{A,ij}|M_E,R_E}$ with itself of order $\tilde{N}_{A,D}$. The expected number of

aftershocks for some $\{M_E, R_E\}$ pairs is given in Figure 4.11, while Figure 4.12 reports the distributions of damage in the corresponding aftershock sequences.
These distributions allow to compute, via Equation (4.15), the distribution of the damage accumulated over the cluster, that is integrating over $\{M_E, R_E\}$.

The $P[\Delta\mu_i > \delta\mu]$ obtained is compared in Figure 4.13 with the distribution obtained when the contribution of aftershocks is neglected, that is with the results of Equation (4.8) in terms of complementary cumulative distribution function (CCDF).
Changes in probability in the case the aftershock sequences are accounted for are depicted in Figure 4.14. Note that the distribution of damage in the cluster, Equation (4.35), is characterized by a probability mass in zero, as not all clusters are damaging, this accounts for the chance that the mainshock and all aftershocks are undamaging.
For the considered example, the probability that the cluster is undamaging is $P_i^0 = 1 - P[\Delta\mu_i > 0] = 0.62$, which implies the rate of damaging clusters to be $\lambda_D = \lambda \cdot P[\Delta\mu_i > 0] = 0.013 \cdot 0.38 = 0.005[events/yr]$.
For comparison it may be worth to report also about the probability that the mainshock only is undamaging, which is $P_{E,i}^0 = 0.65$, marginally with respect to $\{M_E, R_E\}$.

$$P[\Delta\mu_i \le \delta\mu] = \begin{cases} P_i^0 & \delta\mu = 0 \\ P_i^0 + \int_0^{\delta\mu} f_{\Delta\mu_i}(z) \cdot dz & \delta\mu > 0 \end{cases} \tag{4.35}$$

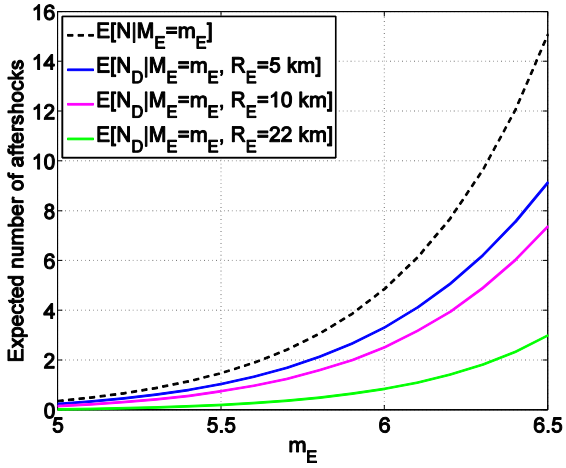

Figure 4.11. Expected number of total and damaging aftershocks conditional to the features of the mainshock.

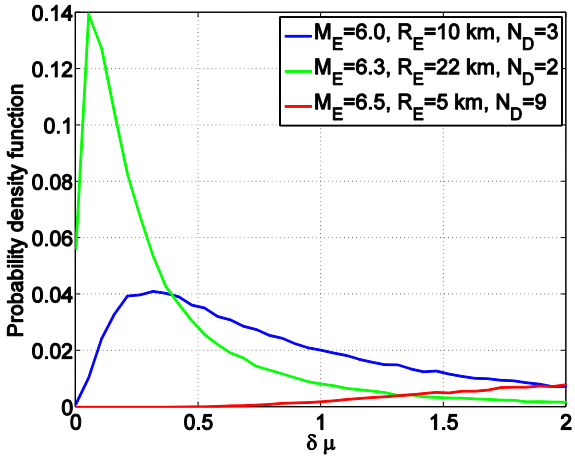

Figure 4.12. Distribution of cumulated damage in aftershock sequences (obtained via Monte Carlo simulation) conditional to some mainshock cases.

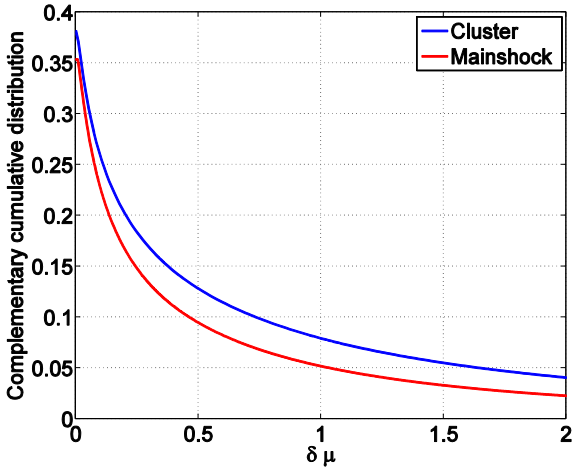

Figure 4.13. CCDFs of damage increment in the cluster and in the mainshock only.

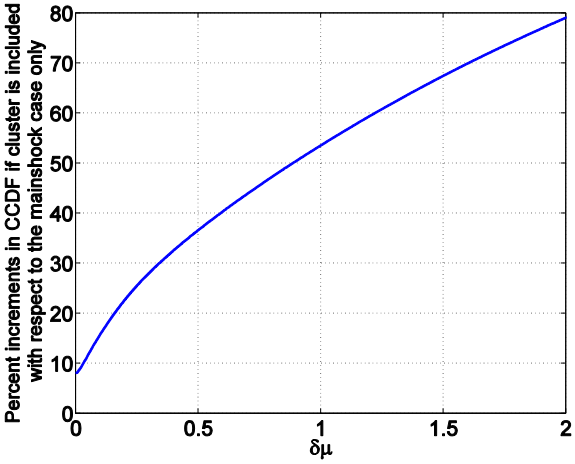

Figure 4.14. Percent probability increments if the aftershock sequence effect is not neglected.

4.6.4. Results of reliability assessment

The distribution of damage in the cluster, $P\left[\Delta\mu_i > \delta\mu\right]$, given that the cluster is damaging, was then alternatively approximated via a gamma and an inverse-Gaussian distribution. It was anticipated that the damage RV is not continuous.
Indeed, it has a probability mass at zero accounting for the non-damaging clusters, which cannot be modeled by the gamma and inverse-Gaussian distributions; therefore, these continuous RVs have been adopted to approximate only the continuous part of the damage in Equation (4.35) (whose area is normalized to one).
The criterion to calibrate the parameters of these two distributions was to set their mean and variance the same as that of the damage conditional to the occurrence of a damaging cluster. These mean and variance are equal to 0.77 and 2.18, respectively. The corresponding parameters are given in Table 4.1.

Table 4.1. Parameters of the gamma and of the inverse Gaussian distributions.

Gamma		**Inverse-Gaussian**	
γ_D	α_D	η_D	ν_D
0.3556	0.2762	0.2145	0.7766

At this point it is possible to compute the CDF of the lifetime of the structure, $F_T(t)$.
In fact, Figure 4.15 shows such distribution computed in different cases:
according to Equation (4.18) and Equation (4.21), that is (i) when the distribution of damage in the cluster is assumed to follow a G or an IG distribution respectively, and the expected number of damaging clusters is considered; (ii) when the distribution of damage in the cluster is assumed to follow a G or an IG distribution, yet the approximation of the expected number of damaging clusters relaxed, that is reliability

is computed by means of Equation (4.3) where the probability of the sum of damages exceeding the threshold refers to G and IG approximations; (iii) without any approximation other than those yielding the distributions in Figure 4.13 (obtained by means of structural simulation), these structural lifetime distributions refer to both the *cluster* and the *mainshock*, and where computed applying Equation (4.3).

The cluster simulation curve is a reference case, as it is the case without any approximating hypothesis. Therefore, Figure 4.16 reports on the ratios of the failure probabilities reported in Figure 4.15 as a function of time and with respect to this case. For example, the ratio of the probabilities from the $simulation_{mainshock}$ to those from the $simulation_{cluster}$ curve, allows appreciating the significance, in the considered example, of accounting for the potential damage effect of aftershocks in the cluster. Similar, the ratios of the other curves allow to evaluate the effect of the approximations considered, that is when damage is modeled by a G or an IG RV and also when the number of occurring clusters is replaced by the expected value of those damaging. Obtained results show that considering the mainshock only leads to an appreciable un-conservative estimate of failure probability, and that the considered approximations, generally lead to acceptable errors, at least in the range of low failure probabilities, of largest civil engineering interest. At least in this application, the G approximation of cluster damage seems to provide better results than the IG.

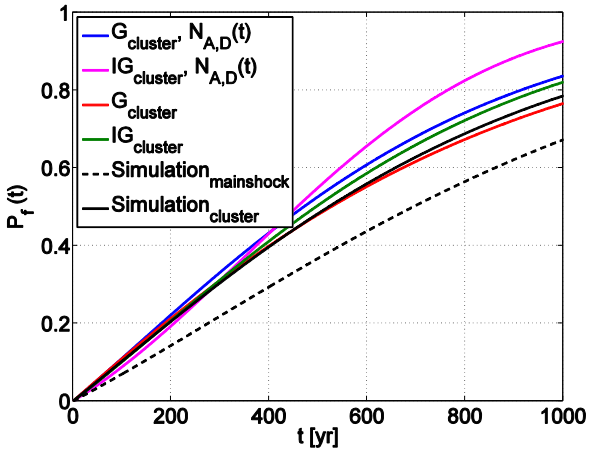

Figure 4.15. Lifetime distributions accounting for the cluster effect with different degrees of approximation along with that when only mainshocks are considered.

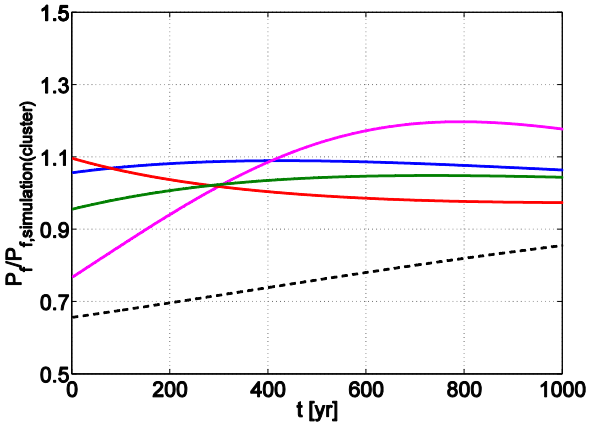

Figure 4.16. Ratio of failure probabilities from curves in the above figure to the reference case that is simulation$_{cluster}$.

Finally, Table 4.2 reports about examples of conditional failure probabilities as per section 4.5.3. In particular, the following cases were considered: (i) failure probability in 50 yr when at 25 yr 0.7 residual capacity is measured, from Equation (4.22) and Equation (4.23); (ii) failure probability in 50 yr when at 25 yr it is observed that the

structure hasn't failed yet, from Equation (4.25) and Equation (4.26); (iii) failure probability in 50 yr when at 25 yr it is observed that the structure hasn't failed yet, and it is known that it has suffered one damaging earthquake, from Equation (4.28) and Equation (4.29). It is confirmed, at least referring to this application, that approximations introduced are tolerable and that the G distribution performs better than the IG.

Table 4.2. Conditional failure probabilities for different knowledge levels.

	Simulation	**Gamma**	**Inverse-Gaussian**
$P\left[D(50) \geq \bar{\mu} \middle| D(25) = 0.3 \right]$	0.0335	0.0359	0.0281
$P\left[D(50) \geq \bar{\mu} \middle| D(25) < 1 \right]$	0.0263	0.0282	0.0219
$P\left[D(50) \geq \bar{\mu} \middle| D(25) < 1 \cap k_D = 1 \right]$	0.0347	0.0357	0.0354

4.7. Conclusions

Starting from: classical stochastic modeling of mainshocks occurrence, conditional process modeling of aftershock sequences, and a probabilistic structural damage accumulation model, life-cycle reliability of constructions subjected to seismic clusters was addressed. The developed model, consistent with the classical framework of performance-based earthquake engineering, assumes that the occurrence of seismic clusters may be described by the same homogeneous Poisson process characterizing mainshock occurrence, while aftershocks' occurrence follows a non-homogeneous Poisson process based on the modified Omori-law, and therefore is conditional on mainshock magnitude.

The structural damage model postulated leads damage increments in different mainshocks to be independent and identically distributed; damage increments in aftershocks pertaining to a specific mainshock are also independent and identically distributed random variables, given the mainshock features. This allowed to formulate

the distribution of damage in a generic cluster, which is also i.i.d. with respect to other clusters. These characteristics of the cluster-damage distribution enable to formulate the non-negative damage accumulation process, which in turn, under the additional hypotheses that damage is a gamma or (as an alternative) an inverse-Gaussian RV, allowed closed-form solution, even if approximate, for the life-cycle reliability assessment. Finally strategies are also formulated which allow to use additional information about the status of the structure at the time of the assessment in order to perform state-dependent reliability evaluations.

A simple application was set-up with a two-fold aim: (i) to appreciate the effect of changes in reliability assessment when the effect of virtually damaging aftershock sequences are not neglected, and (ii) to evaluate the tolerability of the adopted approximated closed-forms. An elastic perfectly plastic single-degree-of-freedom system located in a generic seismogenic areal source was considered, spatial distribution of aftershocks was modeled by a semi-empirical relationship function of mainshock magnitude and location. Then, distributions of intensities in mainshocks and in following sequences were obtained. Integration of those with the results of seismic demand analysis for the considered structure, led to the distribution of damage in mainshocks, aftershocks and, finally, in the single (generic) cluster. This distribution, conditional to damage larger than zero, was fitted by the mentioned reproductive models calibrated to retain mean and variance of damage computed via structural analysis. Results show that, at least in the examined case, the contribution of aftershocks to the life-cycle assessment of earthquake-resistant structures may be not negligible, yet the problem may be addressed via stochastic modeling consistent with PBEE, which may lead to convenient closed-form approximations.

References

Ambraseys NN, Simpson KA and Bommer JJ (1996). Prediction of horizontal response spectra in Europe. *Earthquake Eng. Struct. Dyn.* 25: 371-400.

Boyd OS (2012). Including foreshocks and aftershocks in time-independent probabilistic seismic hazard Analyses. *B. Seism. Soc. Am.* 102(3): 909-917.

Cornell CA, Krawinkler H (2000). Progress and challenges in seismic performance assessment. *Peer Center Newletter* 3(2).

Cosenza E, Manfredi G (2000). Damage indices and damage measures. *Prog. Struct. Eng. Mat.* 2(1): 50-59.

Giorgio M, Guida M, Pulcini G (2010). A state-dependent wear model with an application to marine engine cylinder liners. *Technometrics* 52(2): 172-187.

Gruppo di Lavoro (2004). *Redazione della Mappa di Pericolosità Simica Prevista dall'Ordinanza PCM 3274 del 20 Marzo 2003, Rapporto conclusivo per il Dipartimento della Protezione Civile*. Istituto Nazionale di Geofisica e Vulcanologia, Rome, Italy. (In Italian)

Gutenberg R, Richter CF (1944). Frequency of earthquakes in California. *B. Seism. Soc. Am.* 34(4): 185-188.

Iervolino I, Galasso C, Cosenza E (2010). REXEL: computer aided record selection for code-based seismic structural analysis. *B. Earthq. Eng.* 8(2): 339-362.

Iervolino I, Giorgio M, Chioccarelli E (2013a). Gamma degradation models for earthquake resistant structures. *Struct. Saf.* 45: 48–58.

Iervolino I, Giorgio M, Chioccarelli E (2013b). Closed-form aftershock reliability of damage-cumulating elastic-perfectly-plastics- ystems. *Earthquake Eng. Struct. Dyn.* http://dx.doi.org/10.1002/eqe.2363 (in press)

Iervolino I, Giorgio M, Chioccarelli E (2013c). Gamma modelling of aftershock reliability of elastic-perfectly-plastic systems. Proc. of *Vienna Congress on Recent Advances in Earthquake Engineering and Structural Dynamics* (VEESD) – Vienna, Austria.

Iervolino I, Giorgio M, Polidoro B (2013d). Probabilistic seismic hazard analysis for

seismic sequences. Proc. of *Vienna Congress on Recent Advances in Earthquake Engineering and Structural Dynamics* (VEESD) – Vienna, Austria.

Iervolino I, Giorgio M, Polidoro B (2014). Sequence-based probabilistic seismic hazard analysis. *B. Seism. Soc. Am.* (in press)

Johnson NL, Kotz S, Balakrishnan N (1994). *Continuous univariate distributions*. Vol. 1, Wiley Series in Probability and Mathematical Statistics: Applied Probability and Statistics (2nd ed.), John Wiley & Sons, New York.

Joyner WB and Boore DM (1981). Peak horizontal acceleration and velocity from strong motion records including records from the 1979 Imperial Valley, California, earthquake. *B. Seism. Soc. Am.* 71(6): 2011-38.

Lolli B, Gasperini P (2003). Aftershocks hazard in Italy Part I: Estimation of time-magnitude distribution model parameters and computation of probabilities of occurrence. *J. Seismol.* 7(2): 235-257.

Luco N, Cornell CA (2007). Structure-specific scalar intensity measures for near-source and ordinary earthquake ground motions. *Earthq. Spectra* 23(2): 357-392.

Luco N, Gerstenberger M, Uma S, Ryu H, Liel A, Raghunandan M (2011). A methodology for post-mainshock probabilistic assessment of building collapse risk. Proc. of the *9th Pacific Conference on Earthquake Engineering*, Auckland, New Zealand.

Matthews VM, Ellsworth LW, Reasenberg AP (2002). A Brownian model for recurrent earthquakes. *B. Seism. Soc. Am.* 92(6): 2233-2250.

McGuire RK (2004). Seismic hazard and risk analysis. *Earthquake Engineering Research Institute*, MNO-10, Oakland, CA.

Oehlert GW (1992). A note on the delta method. *The American Statistician* 46(1): 27-29.

Park Y, Ang A (1985). Mechanistic seismic damage model for reinforced concrete. *J. Struct. Eng.-ASCE* 111(4): 722-739.

Ross SM (1996). *Stochastic Processes*, 2nd edn. Wiley Series in Probability and Statistics: Probability and Statistics, John Wiley & Sons, New York.

Sanchez-Silva M, Klutke G-A, Rosowsky DV (2011). Life-cycle performance of

structures subject to multiple deterioration mechanisms. *Struct. Saf.* 33(3): 206-217.

Utsu T (1961). A statistical study on the occurrence of aftershocks. *Geophys. Mag.* 30: 521–605.

Utsu T (1970). Aftershocks and earthquake statistics (1): Some parameters which characterize an aftershock sequence and their interrelations. *Journal of the Faculty of Science*, Hokkaido University, Series 7, Geophysics 3(3): 129-195.

Vamvatsikos D, Cornell CA (2002). Incremental dynamic analysis. *Earthquake Eng. Struct. Dyn.* 31(3): 491-514.

Yeo GL, Cornell CA (2005). *Stochastic characterization and decision bases under time-dependent aftershock risk in performance-based earthquake engineering*, PEER Report 2005/13, Pacific Earthquake Engineering Research Center, Berkeley, CA, USA.

Yeo GL, Cornell CA (2009a). A probabilistic framework for quantification of aftershock ground-motion hazard in California: Methodology and parametric study. *Earthquake Eng. Struct. Dyn.* 38: 45-60.

Yeo GL, Cornell CA (2009b). Building life-cycle cost analysis due to mainshock and aftershock occurrences. *Struct. Saf.* 31(5): 396-408.

Chapter 5 - SUMMARY AND CONCLUSIONS

5.1. Summary and conclusions

The current best practice with respect to long-term seismic risk analysis of structures is represented by the performance-based earthquake engineering framework proposed by Pacific Earthquake Engineering Research Center. In particular, the performance assessment and the design process used to evaluate the seismic risk is divided into four steps, consisting of quantifying the seismic ground motion hazard, assessing the structural response, estimating the damage to building and contents and resulting consequences in terms of financial losses, fatalities and business interruption. All previous components are usually considered to be time-invariant; however, variation in time of seismic structural risk may involve all components that form the performance-based earthquake engineering framework. This thesis mainly focused on the time-variant aspects that can involve both the hazard and the life-cycle assessment of structures, highlighting in both cases, the aftershock contribution.

Referring to the probabilistic seismic hazard analysis (PSHA), most of the studies related to seismicity and seismic hazard assessment are based on time-independent models. In fact, traditional PSHA uses the homogeneous Poisson process (HPP) which is a stationary-increment memory-less model; that is, the number of events depends only on the length of the considered time interval and it is independent of the starting time and the number of events happened before. Such a model is especially suitable when several (independent) sources contribute to the seismic threat. However, when a single fault is of concern and/or the time scale is different from that of the long term, other models may better represent random earthquakes generation.

Chapter 2 provided a brief review of the most important assumptions of some history-dependent processes underlining differences in terms of analytical hypotheses and physical interpretations. Attention was focused on two types of processes, available in literature, that model earthquakes occurrence.

The first typology considered was that of *renewal processes*, which usually applies when *characteristic* earthquakes are of concern, that is, when the considered source tends to produce a single magnitude events. Within this category, the reviewed models were: the Brownian Passage Time; a renewal process with Erlang (i.e., Gamma with integer shape parameter) interarrival time distribution; and finally, a model in which it is assumed that an inverted Gamma distribution represents the interarrival time.

Differently from the above models, the second category reviewed allows to include a relationship between the time and the magnitude of the earthquake, both are considered as random variables. Two models were reviewed: the *time-predictable* and the *slip-predictable* models.

As an illustrative application, the Paganica fault (in central Italy; believed to be the source of the 2009 L'Aquila earthquake) and a site close to it were considered to compute both the probability of observing one event in the time interval of interest, and the seismic hazard, in terms of ground motion intensity measure as a function of the time elapsed since the last earthquake. Examples also included, as a benchmark, hazard when HPP is considered. The magnitude was considered to be that of characteristic events. To render homogeneous all models, these were calibrated so that the interarrival time distributions had the mean and variance as similar as possible. Considering the time intervals of common engineering interest, it was assumed that the probability of more than one event was negligible (showed for the Erlang renewal process), simplifying hazard calculations. It was also observed that as the hazard-rate function, some processes show a decreasing probability of occurrence after a certain time since the last event.

Engineering hazard analysis showed that history-dependent models have a similar trend, especially renewal processes, until a time of about a half of the mean return period of the event, and that the results from all models tend to relatively diverge with the increasing elapsed time since the last event. This means that the longer is the time spent since the last known earthquake on the source, the more critical is the selection of the process which is considered to be appropriate to represent earthquake occurrence.

Traditional PSHA only refers to the occurrence of mainshocks, that is, prominent magnitude earthquakes possibly identified within a sequence of events concentrated both in space and time (i.e., clusters). Within the sequence, according to some models, aftershocks may be seen as triggered by the mainshock. The features of each sequence depend only on the magnitude and location of the triggering event, being conditionally independent (in stochastic sense) of the history. Starting from these premises, some authors put their attention on aftershocks occurrence, in particular on the ground motions that they may produce causing weakening and/or collapse of structures perhaps already damaged (but not yet repaired) by the mainshock. In this context, they developed the aftershock-PSHA to evaluate the aftershock hazard expressed in terms of probability of exceedance of a ground motion intensity measure threshold. Starting from these studies, in **Chapter 3**, it was shown how it is possible to analytically combine results of PSHA and APSHA to get a probabilistic seismic hazard analysis for mainshock-aftershocks seismic sequences (SPSHA). The model was built on the hypotheses that the occurrence of clusters is probabilistically described by the same stochastic counting process of the main events. Within the cluster, the occurrence of mainshock is regulated by a HPP, while occurrence of aftershocks is regulated by a non-homogeneous Poisson process (NHPP) with a rate, which depends on the magnitude of the triggering mainshock.
As an illustrative application, a generic seismogenic source was considered and the SPSHA expressed in terms of annual rate of exceedance of different intensity measure levels was computed and compared to the classical PSHA results. The SPSHA was compared, both in terms of rates given the *IM* threshold, and in terms of *IM* given the return period. Results of the illustrative application presented helped to assess the increase in seismic hazard also considering aftershock contribute. In fact, at least for the considered case, it appeared changes up to about 30% in PGA rate and up to about 10% in pseudo-spectral acceleration values corresponding to the 475 yr return period.

Finally, accounting still for the effect of the whole cluster, in **Chapter 4**, a stochastic life-cycle damage accumulation model for earthquake resistant structures was developed. Earthquake clusters were considered instantaneous with respect to

structural life; therefore, seismic events were described by a marked point process, where each event was represented by its occurrence time (i.e., the occurrence time of the triggering mainshock) and damage that it produces. In particular, it was assumed that the occurrence of earthquake clusters was regulated by a HPP characterized by the same rate considered for the mainshocks (as in Chapter 3).

The model presented, considers that the structure may suffer damage both in the mainshock and in the following aftershocks and that not all events are strong enough to damage it. Moreover, considering an elastic-perfectly-plastic single-degree of freedom system, it was assumed that increments of damage accumulated over different seismic sequences are independent and identically distributed random variables, which are also independent of the process regulating occurrence of clusters. These last assumptions were also used to describe the cumulative damage in the single cluster, where it was assumed that aftershocks occurrence follows a NHPP.

Starting from the above hypothesis, the cumulative probability function of structural lifetime was formalized. It was also added the case in which damage in a single event was susceptible of gamma and inverse Gaussian representation whose reproductive property allowed, when event occurrence follows a HPP process, a closed- and/or approximate-form solutions for absolute and conditional reliability problems.

As an illustrative application, an elastic-perfectly plastic single degree of freedom structure located in an ideal seismic source zone was considered to appreciate the effect of changes in reliability assessment when the aftershock contribute is considered, and to evaluate the tolerability of the adopted approximated closed-forms. In particular, spatial distribution of aftershocks was modeled by a semi-empirical relationship function of mainshock magnitude and location. Then, distributions of intensities in mainshocks and in following sequences were obtained. Integration of those with the results of seismic demand analysis for the considered structure, led to the distribution of damage in mainshocks, aftershocks and, finally, in the single (generic) cluster. This distribution, conditional to damage larger than zero, was fitted by the gamma and inverse Gaussian distributions calibrated to retain mean and variance of damage computed via structural analysis. The life-cycle assessment was hence compared with the case damaging aftershock effect was ignored.

Starting from the closed-form solutions, which provided the absolute (i.e., aprioristic) probability that a new structure fails in a time interval of interest, conditional failure probabilities, which account for information possibly available at the epoch of the evaluation, were calculated. Results showed that, at least in the examined case, the contribution of aftershocks to the life-cycle assessment of earthquake-resistant structures may be not negligible and that the considered approximations, generally lead to acceptable errors, at least in the range of low failure probabilities, of largest civil engineering interest. At least in the developed application, the gamma approximation of cluster damage seemed to provide better results than the inverse Gaussian.